





RESEARCH ARTICLE

An isotopic approach to partition evapotranspiration in a mixed deciduous forest

Phoebe G. Aron¹  | Christopher J. Poulsen¹  | Richard P. Fiorella²  |
Ashley M. Matheny³  | Timothy J. Veverica⁴

¹Department of Earth and Environmental Sciences, University of Michigan, Ann Arbor, MI, 48109, USA

²Department of Geology and Geophysics, University of Utah, Salt Lake City, UT, 84112, USA

³Department of Geological Sciences, Jackson School of Geosciences, University of Texas, Austin, TX, 78712, USA

⁴University of Michigan Biological Station, University of Michigan, Pellston, MI, 49769, USA

Correspondence

Phoebe G. Aron, Department of Earth and Environmental Sciences, University of Michigan, Ann Arbor, MI 48109, USA.
Email: paron@umich.edu

Funding information

National Science Foundation Hydrological Science, Grant/Award Number: 1521238; National Science Foundation Macrosystems Biology Early Neon Science, Grant/Award Number: 1802880; National Science Foundation Tectonics Program, Grant/Award Number: 1550101; University of Michigan Department of Earth and Environmental Sciences Rackham Graduate School University of Michigan Biological Station

Abstract

Transpiration (T) is perhaps the largest fluxes of water from the land surface to the atmosphere and is susceptible to changes in climate, land use and vegetation structure. However, predictions of future transpiration fluxes vary widely and are poorly constrained. Stable water isotopes can help expand our understanding of land-atmosphere water fluxes but are limited by a lack of observations and a poor understanding of how the isotopic composition of transpired vapour (δ_T) varies. Here, we present isotopic data of water vapour, terrestrial water and plant water from a deciduous forest to understand how vegetation affects water budgets and land-atmosphere water fluxes. We measured subdiurnal variations of $\delta^{18}\text{O}_T$ from three tree species and used water isotopes to partition T from evapotranspiration (ET) to quantify the role of vegetation in the local water cycle. We find that $\delta^{18}\text{O}_T$ deviated from isotopic steady-state during the day but find no species-specific patterns. The ratio of T to ET varied from 53% to 61% and was generally invariant during the day, indicating that diurnal evaporation and transpiration fluxes respond to similar atmospheric and micrometeorological conditions at this site. Finally, we compared the isotope-inferred ratio of T to ET with results from another ET partitioning approach that uses eddy covariance and sap flux data. We find broad midday agreement between these two partitioning techniques, in particular, the absence of a diurnal cycle, which should encourage future ecohydrological isotope studies. Isotope-inferred estimates of transpiration can inform land surface models and improve our understanding of land-atmosphere water fluxes.

KEYWORDS

eddy covariance, evapotranspiration, forest hydrology, partitioning, sap flux, water cycle, water isotopes

1 | INTRODUCTION

Evapotranspiration (ET) connects the water and carbon cycles and plays an important role maintaining terrestrial energy balance (Dunn & Mackay, 1995; Ellison et al., 2017; Swann, Fung, & Chiang, 2012; Worden, Noone, & Bowman, 2007). Despite its broad significance, estimates of terrestrial water fluxes from

reanalysis, upscaled observations and land surface models (LSMs) differ by up to 50%, and predicting future land-atmosphere water fluxes remains a challenge (Mao et al., 2015; Mueller et al., 2013; Vinukollu, Meynadier, Shef, & Wood, 2011). Central to this uncertainty are yet unresolved responses of plants to climate and land use change (Frank et al., 2015; Jackson et al., 2001; Massmann, Gentine, & Lin, 2019; Schlesinger & Jasechko, 2014). In a higher

CO₂ world, some predict that changes to leaf area index (LAI), stomatal conductance, soil moisture and terrestrial run-off will intensify the water cycle (Brutsaert, 2017; Ohmura & Wild, 2002; Zeng et al., 2018; Zhang et al., 2016); others anticipate that these vegetation-induced changes will decrease water cycling (Gedney et al., 2006; Labat, Godd, Probst, & Guyot, 2004). Consequently, a growing body of eco-hydrological research is aimed at studying terrestrial water fluxes to better understand what drives water exchange between the land and the atmosphere, and how terrestrial hydrology may change in the future and how plants regulate freshwater resources.

ET is composed of ecosystem evaporation (E, including surface evaporation and evaporation of canopy-intercepted water) and plant transpiration (T). The ratio of T to ET, hereafter referred to as F_T , provides insight into the role that vegetation plays in terrestrial water recycling and links plant hydrology with climate and meteorological conditions (Stoy et al., 2019). A complete understanding of this ratio is an important step towards predicting how plants will respond to land use and climate changes and how hydrologic balance may change in the future. To date, there is no consensus about the values of global, regional and ecosystem F_T (Anderegg, Trugman, Bowling, Salvucci, & Tuttle, 2019; Bowen, Cai, Fiorella, & Putman, 2019; Stoy et al., 2019). In particular, estimates of T and F_T from LSMs and remote sensing algorithms, which rely on ecosystem-scale information, do not currently agree with ground-based observations of T and F_T that can vary on spatial scales of less than a kilometre (Good, Noone, & Bowen, 2015; Talsma et al., 2018; Wei et al., 2017). Most LSMs and remote sensing data cannot capture subgrid cell variations of lateral water flow (Chang et al., 2018; Ji, Yuan, & Liang, 2017; Maxwell & Condon, 2016), plant water stress (Fang et al., 2017; Matheny, Bohrer, Stoy et al., 2014) and micrometeorological forcing (Badgley, Fisher, Jimenez, Tu, & Vinukollu, 2015), which are necessary to accurately model F_T . Further complicating our understanding of land-atmosphere water exchange, some ground-based observations of ET may not actually capture conditions at the transpiring or evaporating surfaces. For example, near-surface gradients of water vapour concentrations and vapour pressure deficits (VPDs) can make it difficult to relate ET measurements, most of which are made using eddy covariance above canopies, to leaf and soil fluxes within canopies (Aron, Poulsen, Fiorella, & Matheny, 2019; De Kauwe, Medlyn, Knauer, & Williams, 2017; Jarvis & McNaughton, 1986). Therefore, additional leaf- and soil-level flux measurements are needed to improve estimates of F_T and predictions of terrestrial water fluxes.

Stable water isotopes can improve our understanding of water fluxes from the land to the atmosphere because the component processes, evaporation and transpiration, have distinct isotopic signatures (Yakir & Sternberg, 2000). Evaporation causes a large fractionation that enriches vapour in the lighter isotope. Because plants generally do not fractionate water during uptake and a vast amount of water passes through plants without fractionating, transpiration generally adds vapour with a higher proportion of heavy isotopes to the atmosphere (Ehleringer & Dawson, 1992). Using these fingerprints, many researchers have used water isotopes to measure F_T and learn about

land-atmosphere water exchange (Xiao, Wei, & Wen, 2018 and references therein).

Isotopic ET partitioning requires knowledge of the isotope ratios associated with ET (δ_{ET}), evaporation (δ_E), and transpiration (δ_T). Until recently, isotope-inferred estimates of ET were limited to a low temporal resolution (day-to-annual timescales). As a result, the isotopic composition of transpired vapour was not measured and instead was assumed to be in isotopic steady-state (equal to that of source water) (Haese, Werner, & Lohmann, 2013). However, observations from high-resolution laser absorption spectrometers now enable estimates of δ_T and show that transpiration can deviate from isotopic steady-state when periods of stable environmental conditions are too short to allow δ_T to reach the isotopic composition of source water (Dubbert et al., 2014; Dubbert, Cuntz, Piayda, Maguás, & Werner, 2013; Dubbert, Cuntz, Piayda, & Werner, 2014; Dubbert, Kübert, & Werner, 2017; Simonin et al., 2013). These δ_T observations may improve estimates of land-atmosphere water fluxes and our understanding of the role plants play in the water cycle. However, thus far studies of δ_T have focused only on a small subset of species and environments, and it is still quite challenging to model short-term (subdiurnal) variations of δ_T (Dubbert, Cuntz, et al., 2014) or incorporate nonsteady-state transpiration into isotope-enabled LSMs (Wong, Nusbaumer, & Noone, 2017). Additional observations of δ_T from a wide variety of species and environments can inform estimates of F_T and may help reconcile F_T differences between observations and LSMs or remote sensing.

Forests play a critical role in land-atmosphere water exchange, but very few studies have directly used water isotopes to partition forest ET (Lai, Ehleringer, Bond, & Paw, 2006; Lee, Kim, & Smith, 2007; Moreira et al., 1997). Instead, most isotopic ET partitioning studies are based in croplands or grasslands where water management is easy to control and canopy cover is low, uniform and continuous (e.g., Aouade et al., 2016; Lu et al., 2017; Wu, Du, Ding, Tong, & Li, 2017). To address this gap, we measured the isotopic composition of transpired vapour from three tree species, bigtooth aspen (*Populus grandidentata*), red oak (*Quercus rubra*) and red maple (*Acer rubrum*), in a mixed deciduous forest in northern lower Michigan. We then use δ_T measurements to estimate forest F_T . Our objectives are to (1) quantify the temporal and species-specific variability of δ_T , (2) use water isotopes to estimate forest F_T and (3) evaluate whether measurements of nonsteady-state δ_T improve isotopic ET partitioning. Finally, we compare our results from the isotopic ET partitioning with results from another partitioning technique that uses eddy covariance and sap flux data. Taken together, these objectives examine whether water isotopes provide accurate quantitative estimates of forest ET fluxes. If so, isotope-inferred F_T and δ_T may inform isotope-enabled LSMs and improve predictions of land-atmosphere water exchange. Broadly, this work builds upon a growing field of high-resolution isotope ecohydrology studies that seek to understand the role of vegetation in local, regional and global water budgets.

2 | ET PARTITIONING

2.1 | Theoretical isotopic ET flux partitioning

The isotopic two-source model is commonly used to partition evapotranspiration (ET) because evaporation (E) and transpiration (T) fluxes have distinct isotopic compositions. In this framework, ET is defined as

$$ET = E + T. \quad (1)$$

Following isotopic mass balance and using delta (δ) notation, Equation 1 can be expressed as

$$\delta_{ET}ET = \delta_E E + \delta_T T \quad (2)$$

where δ_{ET} , δ_E and δ_T are the isotopic compositions of ET, evaporation and transpiration, respectively. A list of all symbols and abbreviations used in this study is presented in Table 1. Throughout this manuscript, we use δ notation in per mil (‰), where R is the ratio of the heavy isotope to the light isotope ($\delta = (R_{\text{sample}}/R_{\text{standard}} - 1) \times 1,000$) and the standard is Vienna Standard Mean Ocean Water (VSMOW) (Coplen, 1996; Gat, 1996). Combining Equation 1 and Equation 2 yields F_T , the ratio of T to ET:

$$F_T = \frac{T}{ET} = \frac{\delta_{ET} - \delta_E}{\delta_T - \delta_E}. \quad (3)$$

This linear, two-source mixing model has been used in a number of previous studies to partition water fluxes of ET (e.g., Wang & Yakir, 2000; Xiao et al., 2018; Yakir & Sternberg, 2000).

We determined δ_{ET} with a Keeling mixing model (Keeling, 1958; Yakir & Sternberg, 2000), where δ_{ET} is estimated as the y-intercept of

a linear regression between the isotopic composition of atmospheric water vapour (δ_a) and the reciprocal of the water vapour concentration.

The isotopic composition of transpired vapour (δ_T) is calculated from leaf chamber measurements following Wang, Good, Caylor, and Cernusak (2012). Using this approach, δ_T is defined as

$$\delta_T = \frac{q_m \delta_m - q_a \delta_a}{q_m - q_a}, \quad (4)$$

where q is the water vapour concentration, $_m$ refers to measurements when the chamber was closed around a leaf, and $_a$ refers to measurements when the chamber was open to ambient vapour (Wang et al., 2012).

The isotopic composition of soil evaporation (δ_E) is estimated using the Craig and Gordon (1965) model:

$$\delta_E = \frac{\alpha_{eq}^{-1} \delta_s - h \delta_a - \epsilon_{eq} - (1-h) \epsilon_k}{(1-h) + 10^{-3} (1-h) \epsilon_k}, \quad (5)$$

using meteorological measurements and isotopic values of soil water (δ_s) and atmospheric vapour (δ_a). Here, α_{eq} (>1) is the temperature-dependent equilibrium fractionation factor (Majoube, 1971), ϵ_{eq} is calculated as $(1 - 1/\alpha_{eq}) \times 10^3$, ϵ_k is the kinetic fractionation term and h is the relative humidity at the temperature of the evaporating surface.

2.2 | ET partitioning from sap flux and eddy covariance data

ET partitioning from sap flux and eddy covariance measurements follows the approach described by Williams et al. (2004). In this technique, the latent heat-derived ET is separated into biotic (T) and abiotic (E) components using eddy covariance estimates of latent energy and direct measurements of sap flux. To partition ET, we assumed that transpiration accounted for nearly all of the ET fluxes on the driest days

TABLE 1 Description of symbols and subscripts used in this study

Symbol	Description	Subscript	Description
α_{eq}	equilibrium fractionation factor	a	Atmospheric vapour
α_k	kinetic fractionation factor	E	Evaporation
δ	Delta notation, stable isotope value (‰)	ET	Evapotranspiration
$\delta^{18}\text{O}$	Oxygen isotope value (‰)	g	Groundwater
$\delta^2\text{H}$	Hydrogen isotope value (‰)	l	Leaf
d	Deuterium-excess	lake	Lake
E	Evaporation	m	Closed leaf chamber vapour
ET	Evapotranspiration	p	Precipitation
F_T	Transpiration/evapotranspiration	s	Soil
h	Relative humidity	T	Transpiration
q	Specific humidity	x	Xylem
R	Isotope ratio (e.g., $^{18}\text{O}/^{16}\text{O}$)		
T	Transpiration		

during the growing season and derived a scaling equation to estimate the ratio of T to ET on days when evaporation was not negligible (Kool et al., 2014). Additional details on this scaling are provided in the Supporting Information.

3 | METHODS

3.1 | Site description

This study was conducted at the 46-m AmeriFlux-affiliated eddy covariance tower site at the University of Michigan Biological Station (UMBS) in northern lower Michigan (45.59°N, 84.70°W, AmeriFlux database site-ID US-UMB). The forest at this site has been dominated by bigtooth aspen (*P. grandidentata*) and paper birch (*Betula papyrifera*) but is currently transitioning to a mixed composition dominated by red oak (*Q. rubra*), red maple (*Acer rubrum*), white pine (*Pinus strobus*), American beech (*Fagus grandifolia*) and sugar maple (*Acer saccharum*). As a result of heavy logging in the early 20th century, the forest has a relatively uniform age and canopy structure. Mean canopy height is ~22 m and mean peak LAI is 3.9 m² m⁻². The site receives 766 mm of precipitation annually, and the mean annual temperature is 5.5°C (Matheny et al., 2017). Soils at the UMBS site are well-drained Haplorthods of the Rubicon, Blue Lake or Cheboygan series and consist of ~95% sand and ~5% silt (Nave et al., 2011). Additional site details are available in Matheny et al. (2017) and Gough et al. (2013).

3.2 | Isotope measurements

3.2.1 | Surface waters

We collected a variety of surface waters and shallow groundwaters during the 2017 growing season to characterize the isotopic composition of potential source waters for trees and to examine seasonal hydrologic variability near our study site. We collected event-scale precipitation at the tower site in a plastic bucket lined with mineral oil to prevent evaporation (Friedman, Smith, Gleason, Warden, & Harris, 1992; Scholl, Ingebritsen, Janik, & Kauahikaua, 1996). We used a needle point syringe to extract precipitation and avoid transferring any oil to the collection vial. The sampling bucket was cleaned, dried and given a fresh layer of oil between samples. From April to October, we collected monthly samples from the edge of a nearby lake and from the mouth of a groundwater spring. The groundwater spring originates from a seep at the bottom of the lake (Hendricks, Vande Kopple, Goodspeed, & White, 2016). We collected shallow (within 3 m of the surface) groundwater in April, June and November from 15 wells near the mouth of the spring. All liquid water samples were collected in HDPE vials (Wheaton Industries, 986716) and analysed within a few weeks of collection, so we do not expect any fractionation between the plastic HDPE collection containers and the sampled water (Spangenberg, 2012). We used a Picarro L2130-i cavity ringdown spectrometer (CRDS) with an A0211 high-precision

vaporizer and attached autosampler to measure $\delta^{18}\text{O}$ and $\delta^2\text{H}$ of liquid water samples. We used Picarro ChemCorrect software to monitor samples for organic contamination. For liquid samples, precision was better than 0.1‰ and 0.3‰ for $\delta^{18}\text{O}$ and $\delta^2\text{H}$, respectively.

3.2.2 | Vapour

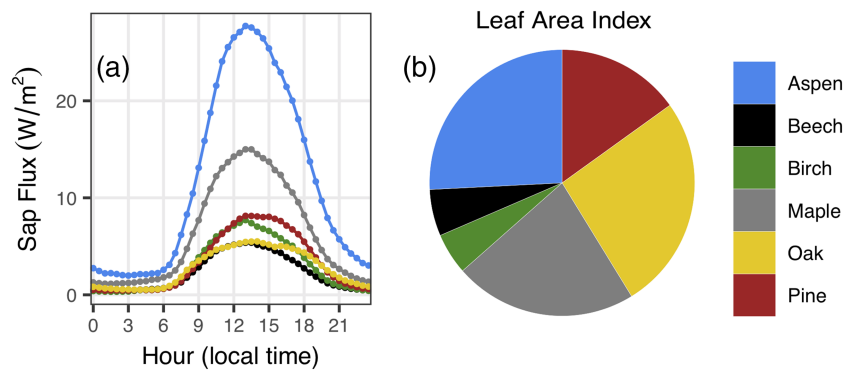
To analyse water vapour isotopes, we deployed two CRDSs, a Picarro L2120-i and a Picarro L2130-i, in a temperature-controlled shed located next to the 46-m eddy covariance tower. We used a Picarro Standard Delivery Module (SDM, A0101) to deliver liquid laboratory standards to monitor for drift and calibrate isotope data to the VSMOW-SLAP scale (Bailey, Noone, Berkelhammer, Steen-Larsen, & Sato, 2015). Each SDM was setup with a Drierite (26800) column and a Picarro high precision vaporizer (A0211) maintained at 140°C and ambient pressure. We analysed standards at night in order to minimize interference with data collection during the day when transpiration was higher.

CRDSs are known to exhibit an isotope-ratio bias due to changes in cavity humidity (Aemisegger et al., 2012). To correct for this bias, we used version 1.2 of the University of Utah vapour processing scripts to derive cavity-humidity correction equations and instrument precision (Fiorella, Bares, Lin, Ehleringer, & Bowen, 2018). We present the 1 σ uncertainty at 10,000 ppmv, the lowest measured vapour mixing ratio, and 25,000 ppmv, near the highest measured mixing ratio. For *d*-excess ($d = \delta^2\text{H} - 8 * \delta^{18}\text{O}$ (Dansgaard, 1964), we assume oxygen and hydrogen errors are independent. 1 σ uncertainty on the L2120-i ranged from 0.28‰ for $\delta^{18}\text{O}$, 0.93‰ for $\delta^2\text{H}$ and 2.45‰ for *d* at 10,000 ppmv to 0.20‰, 0.59‰ and 1.68‰ (for oxygen, hydrogen and *d*, respectively) at 25,000 ppm. On the L2130-i, 1 σ uncertainty ranged from 0.13‰ for $\delta^{18}\text{O}$, 0.43‰ for $\delta^2\text{H}$ and 1.14‰ for *d* at 10,000 ppmv to 0.09‰, 0.29‰ and 0.78‰ (for oxygen, hydrogen and *d*, respectively) at 25,000 ppm. Additional information about the cavity humidity correction equations is available in the Supporting Information.

We installed a vapour sampling manifold on the eddy covariance tower and selected three similarly-sized nearby trees—a bigtooth aspen, a red oak and a red maple—for transpiration measurements. We chose these species because together they account for more than 70% of the LAI and a majority of the sap flux at the site (Figure 1). Leaves and branches from the aspen and oak were accessible from a platform on the eddy covariance tower 15 m above the ground. No maple branches were accessible directly from the eddy covariance tower, so we built a small 5-m tower a few metres from the base of the eddy covariance tower to reach a maple tree. The uppermost extent of all three sampled trees reached the upper canopy and was exposed to full sunlight.

We built two transparent flow-through sampling chambers following the description in Wang et al. (2012) to make δ_T measurements at 5 and 15 m. Each chamber was approximately 20 cm long, 15 cm wide and 5 cm tall. This size accommodated large (up to ~15 cm) oak leaves but was kept small to minimize lag or memory effects between switching samples. Just before a closed-chamber transpiration measurement, we

FIGURE 1 (a) Mean diurnal sap flux (W/m^2) and (b) leaf area index (LAI) by species during the 2017 growing season (May to October)



manually inserted a live leaf (still attached to the tree) into the chamber and sealed the chamber. Each chamber had two small (~ 2 cm) openings to pull in ambient vapour during closed-chamber measurements. The chamber hung from the tree for the duration of each transpiration measurement period. Occasionally, we had to reorient the chamber to prevent the leaf from touching the side of the chamber because any contact points between the leaf and the chamber promoted condensation. Every closed-chamber measurement was made on a different leaf. At the end of the transpiration measurement period, we opened the chamber, removed the leaf and measured ambient vapour from the open chamber.

Sampling lines extended from the chambers to the Picarro analyser. The 5-m chamber had two sampling lines, one to measure vapour when the chamber was closed around a leaf and another to measure vapour when the chamber was open. The 15-m chamber had three sampling lines, one for closed oak measurements, one for closed aspen measurements and one for open chamber measurements. A final ambient-only sampling line extended above the canopy and was collocated adjacent to 34-m meteorological and flux measurements from the eddy covariance tower. All sampling lines were constructed from nonfractionating Bev-A-Line tubing (Simonin et al., 2013), encased in insulation and wrapped with a warm wire to prevent condensation. The whole sampling manifold was held below ambient pressure by a diaphragm pump that operated at ~ 5 L/min to maintain constant airflow and minimize memory effects between samples.

Each Picarro analyser controlled a multiposition valve (VICI/Valco EMT2SD6MWE) to switch between sampling locations. We measured each ambient vapour for 5 min and transpired (closed-chamber) vapour for 10 min. We define a cycle of isotopic measurements as a loop through each port on the multiposition valve and assume that the average isotopic composition at each sampling location represents the isotopic composition at that location for the full cycle of measurements.

Initially, we planned to use the L2120-i to analyse ambient vapour and the L2130-i to analyse transpired vapour. This set-up was designed to measure the highest possible temporal resolution of δ_T . However, the L2130-i analyser malfunctioned after the June sampling campaign, which forced us to reconfigure our approach and use the L2120-i to measure all six locations in August and October. We measured vapour isotopes during three periods in 2017: 19 June (DOY

170); 14 August (DOY 226), 15 August (DOY 227) and 16 August (DOY 228); and 6 October (DOY 279) and 9 October (DOY 282). These days were selected to study transpiration during periods when water fluxes were high (June and August) and low (October). Missing days in October (DOY 280 and 281) are due to technical issues with the Picarro analysers, poor weather and other logistical difficulties at the field site.

3.2.3 | Terrestrial and biological waters

We used a soil auger to collect soil from the top 10 cm around noon on 19 June, 16 August and 6 October. Xylem samples were collected midday at breast height using an increment borer on 16 August, 6 October and 9 October. To avoid disrupting the hydraulics of the trees that were monitored for transpiration, we collected xylem samples from trees near the eddy covariance tower. We collected leaves from the transpiration-monitored trees because leaves from other trees were out of reach and the removal of a few leaves from a fully leafed-out tree was not expected to significantly affect plant hydraulics. Leaf samples were collected around 8 AM, 11 AM, 2 PM and 5 PM on 15 August, 16 August, 6 October and 9 October. To collocate measurements of leaf water and transpired vapour, we collected maple leaves at 5 m and oak and aspen leaves at 15 m. Soil, xylem and leaf samples were stored in a refrigerator after collection.

Waters from soil, xylem and leaf matrices were extracted on a cryogenic vacuum distillation line following the methods of West, Patrickson, and Ehleringer (2006). The midrib was not removed from leaves prior to the distillation. Distilled soil waters were analysed for oxygen and hydrogen isotopes on a Picarro L2130-i as described earlier. Due to complications arising from the presence of organic compounds (West, Goldsmith, Brooks, & Dawson, 2010), leaf and xylem waters were analysed for $\delta^{18}O$ and δ^2H using a Thermo Scientific Delta V gas isotope ratio mass spectrometer (TC/EA-IRMS hereafter) that does not suffer from organic contamination. The TC/EA-IRMS was interfaced with a Thermo Scientific FlashIRMS elemental analyser running in pyrolysis mode. A 0.5- μ l aliquot of distilled water was

injected into a glassy carbon furnace maintained at 1450°C. The product gases were separated chromatographically on a Restek Molesieve 5A column (60/80 mesh, 2 m × 2 mm ID isothermal at 50°C) and were introduced to the IRMS by means of a continuous flow open-split interface (Conflo IV) optimized to each gas for linearity and sensitivity. Each gas was normalized to an injection of internal reference gas, and each batch of samples was then normalized to VSMOW by means of complementary analysis of known standards under these same conditions. Precision of TC/EA-IRMS analyses was better than 0.4‰ for $\delta^{18}\text{O}$ and 2.4‰ for $\delta^2\text{H}$.

3.3 | Sap flux

Sap flux is considered a proxy for transpiration (Granier & Loustau, 1994; Phillips & Oren, 1998). We used a network of custom-built Granier (1987) style thermal dissipation probes in 60 trees to continuously monitor sap flux at our field site. For this project, we installed six additional sap flux probes in the maple and oak trees that were used to measure transpiration to ensure they were hydrologically similar to others at the site. Sap flux measurements were made every minute and reported as 30-min averages. Additional details about the sap flux sensors and network are available in Matheny, Bohrer, Vogel et al. (2014) and Matheny et al. (2017).

3.4 | Meteorological and eddy covariance measurements

Temperature and relative humidity (HMP45g, Vaisala, Helsinki, Finland) were measured at 3, 15 and 34 m from the eddy covariance tower. Three-metre measurements were reported every minute; 15- and 34-m measurements were reported as 30-min averages. To facilitate comparison with other meteorological and eddy covariance data, 3-m temperature and relative humidity were averaged to common 30-min time steps. Daily precipitation amount was measured approximately 6 km east of our field site at the Pellston Regional Airport. These data are available from the National Oceanic and Atmospheric Administration Climate Data Online archive (Network ID USW00014841).

Eddy covariance CO_2 and H_2O fluxes were measured above the canopy at 34 m. The latent heat flux was measured at high resolution (10 Hz) using the eddy covariance approach: water vapour and CO_2 concentrations were measured using a closed-path infrared gas analyser (LI7000, LI-COR Biosciences, Lincoln, NE, USA); wind velocity and temperature were measured with a 3-D ultrasonic anemometer (CSAT3, Campbell Scientific, Logan, UT, USA). The latent heat flux was corrected by the Webb–Pearman–Leuning correction to account for density fluctuations in water vapour fluxes (Webb, Pearman, & Leuning, 1980). A complete description of the eddy covariance data processing is available in Gough et al. (2013). All eddy covariance variables were reported as 30-min averages. Spikes in the eddy covariance data were identified using a median filter (Starkenburger et al., 2016) and removed.

3.5 | Data processing: δ_T calculations and ET partitioning

All isotopic, meteorological and eddy covariance data were processed to a common time step to facilitate analysis. The common time of δ_T measurements was rounded to the nearest half hour of the closed-chamber measurements. Following Equation 4, $\delta^{18}\text{O}_T$ was calculated from isotope and humidity measurements when the chamber was open (measuring ambient vapour) and closed (measuring transpired vapour). The Picarro simultaneously measures isotopic compositions and specific humidity; no additional parameters or measurements are needed to calculate δ_T (Wang et al., 2012). We omit the first 2 min of each measurement period to minimize memory effects from switching sampling ports and used the average of measurements from Minutes 3–5 for the $\delta^{18}\text{O}_T$ calculation (Aemisegger et al., 2012). Although the closed-chamber measurements continued for 10 min, we chose not to use transpired vapour measurements from Minutes 5–10 because we observed that condensation occasionally built up in the chambers after 5 min.

Air within the canopy is usually poorly mixed (Aron et al., 2019), so we used above-canopy measurements for the Keeling regression to derive ecosystem-scale δ_{ET} . In contrast, δ_T measurements are separated by species (e.g., $\delta_{T,\text{maple}}$, $\delta_{T,\text{aspen}}$ and $\delta_{T,\text{oak}}$). At UMBS, maple, aspen and oak account for ~22%, 26% and 26%, respectively, of the total LAI (Figure 1b). To ensure we did not overpredict the transpiration flux from these three species, we scaled $\delta_{T,\text{maple}}$, $\delta_{T,\text{aspen}}$ and $\delta_{T,\text{oak}}$ values by the percentage of total LAI accounted for by each species. This approach can produce species-specific values of F_T , although that is not our focus in this study because similar measurements are already done at UMBS from sap flux data (Figure 1a). Instead, in this study, we combine transpiration fluxes from maple, oak and aspen trees to approximate an ecosystem-wide flux. We refer to F_T calculated from the scaled δ_T measurements as nonsteady-state F_T .

To test the effects of assumed steady-state transpiration on isotope-inferred F_T , we compare nonsteady-state F_T with F_T estimated with two steady-state δ_T assumptions: a source water assumption that uses the Craig and Gordon (1965) leaf water model and defines δ_T as xylem water (δ_x) and a precipitation assumption that sets δ_T as δ_p . A summary of the various techniques and assumptions we use to estimate F_T is presented in Table 2. δ_s and δ_x can vary spatially across a landscape (Brooks, Barnard, Coulombe, & McDonnell, 2010; McDonnell, 2014) and mostly likely reflect a mixture of water from past precipitation events and other incoming surface and groundwater flows (Barbour, 2007). Preferential flow paths through the porous (>90% sand) UMBS soil may also bias the isotopic composition of available soil water (Brooks et al., 2010). Neither the source water nor the precipitation assumptions consider these environmental complexities, and a detailed assessment of soil hydrology is beyond the scope of this study. Instead, the steady-state assumptions used in this study are our best attempt to capture a representative transpiration flux from the forest.

TABLE 2 Summary of F_T methods, species, assumptions and results

Method	Species	Assumptions	F_T explanation	F_T
δ_T measurements (nonsteady-state)	Aspen, maple, oak		Direct leaf-level measurements of δ_T	$37 \pm 2\%$
Source water assumption (steady-state δ_T)	Aspen, maple, oak	$\delta_x = \delta_T$	δ_T scaled to LAI of aspen, maple, oak	$36 \pm 2\%$
Aspen, maple, oak ecohydrologic	Aspen, maple, oak		Sap flux scaled to LAI of aspen, maple, oak	$43 \pm 9\%$ ($40 \pm 7\%$ midday)
Precipitation assumption (steady-state δ_T)	Aspen, beech, birch, maple, oak, pine	$\delta_p = \delta_T$	δ_T scaled to LAI of all non-oak species + $\delta_{x,oak}$ scaled to the LAI of oak ^a	$53 \pm 3\%$,
Plot-level ecohydrologic	Aspen, beech, birch, maple, oak, pine		Total plot level sap flux	$65 \pm 12\%$ ($61 \pm 8\%$ midday)

Abbreviation: LAI, leaf area index.

^aMatheny et al. (2017) demonstrated that oak at our study site has a deeper rooting structure and can access soil water that is more depleted in heavy isotopes than other tree species at the site. As a result, F_T from the precipitation assumption is calculated from the sum of δ_p scaled to the LAI of all non-oak species plus $\delta_{x,oak}$ scaled to the LAI of oak.

4 | RESULTS

4.1 | Seasonal and synoptic-scale variability

Seasonal variations of local meteorology, sap flux and latent heat flux are shown in Figure 2. Temperature, specific humidity, sap flux and latent heat flux increased through the spring, reached a maximum in the summer and decreased in the fall. Soil moisture was greatest in the spring when the soil was moist from winter snowmelt and decreased through the growing season as water percolated through the soil or returned to the atmosphere via ET (Figure 2f). Soil moisture increased rapidly after precipitation events, but due to the high sand content, limited storage potential, and increased ET fluxes after rain, it decreased quickly after each storm pulse (Figure 2f). Sap flux and latent heat were positively correlated (Pearson's $r > 0.75$) throughout the growing season and moderately well correlated with above-canopy VPD ($r > 0.53$) (Figure 2d,e). Imprinted on this seasonal variation, meteorological, eddy covariance and sap flux measurements varied on 3- to 4-day timescales as weather systems passed through the study region (Figure 2). Daily precipitation totals varied from 0 to 1.18 cm (Figure 2f). In general, on rainy days, temperature, sap flux and latent heat were lower, and specific humidity was higher.

Monthly variability of terrestrial (rain, lake, soil and ground) and plant (xylem and leaf) waters $\delta^{18}\text{O}$ and $\delta^2\text{H}$ are shown in Figure 3. Precipitation, surface water and shallow groundwater cluster around the global meteoric water line (GMWL, $\delta^2\text{H} = 8 * \delta^{18}\text{O} + 10\text{‰}$; Craig, 1961). The local meteoric water line (LMWL, $\delta^2\text{H} = 7.9 * \delta^{18}\text{O} + 13.6\text{‰}$) at UMBS has a slope close to the that of the GMWL and an intercept that reflects the high degree of moisture recycling downwind of Lake Michigan (Bowen, Kennedy, Henne, & Zhang, 2012; Putman, Fiorella, Bowen, & Cai, 2019). The isotopic compositions of soil (δ_s), xylem (δ_x) and leaf (δ_l) waters generally fall below the GMWL along lines with shallow slopes ($\sim 2.5\text{‰} \text{‰}^{-1}$) and very low intercepts (approximately -37‰), indicative of evaporative enrichment.

Time series of meteoric water isotopes through the 2017 growing season are shown in Figure 4. Event-scale $\delta^{18}\text{O}_p$ generally varied between -4‰ and -12‰ (-10‰ to -80‰ for $\delta^2\text{H}$), although a large (~ 1.2 cm) storm in late June had a particularly low isotopic composition (-17.1‰ and -120.6‰ for oxygen and hydrogen, respectively, Figure 4a). Precipitation d -excess ($\sim 13\text{‰}$) was relatively consistent from May to October, with the exception of three midsummer storms that had low d -excess ($< 6.1\text{‰}$, Figure 4b). $\delta^{18}\text{O}$ of the lake and groundwater spring, which flows from a seep at the bottom of the lake, increased 1.2‰ and 0.3‰ , respectively, through the growing season (Figure 4a). Together, these trends indicate that some lake water evaporated during the growing season. $\delta^{18}\text{O}$ and $\delta^2\text{H}$ of groundwater was almost always less than that of surface water. The groundwater spring ($\delta^{18}\text{O} -9.1\text{‰}$ to -8.5‰) was therefore likely a mixture of lake water ($\delta^{18}\text{O} -8.1\text{‰}$ to -6.9‰) and shallow groundwater ($\delta^{18}\text{O} -12.2\text{‰}$ to -8.1‰). The seasonal trends in $\delta^{18}\text{O}$ and d -excess of the spring suggest that the contribution of groundwater to the spring decreased through the growing season.

4.2 | Diurnal isotope variability

Soil and xylem waters were evaporatively enriched relative to precipitation on all the days we measured these pools (Figure 5). In August, $\delta^{18}\text{O}_p$ of the rain event just before the measurement period (-9.1‰) was less than that of $\delta^{18}\text{O}_x$ for maple, aspen and oak (-4.2‰ , -6.7‰ and -7.8‰ , respectively) (Figure 5a,b). Similarly, on 6 October, $\delta^{18}\text{O}_p$ (-5.5‰) was lower than $\delta^{18}\text{O}_x$ (-4.8‰ , -4.3‰ and -3.9‰ , maple, aspen and oak, respectively, Figure 5c); on 9 October, $\delta^{18}\text{O}_p$ (-4.7‰) was lower than or nearly equal to $\delta^{18}\text{O}_x$ (-4.9 , -3.4 and -3.3‰ , maple, aspen and oak, respectively, Figure 5d). Precipitation d -excess in August, 6 October and 9 October was higher (14.5‰ , 17.6‰ and 25.2‰ , respectively) than d -excess of xylem water, suggesting that

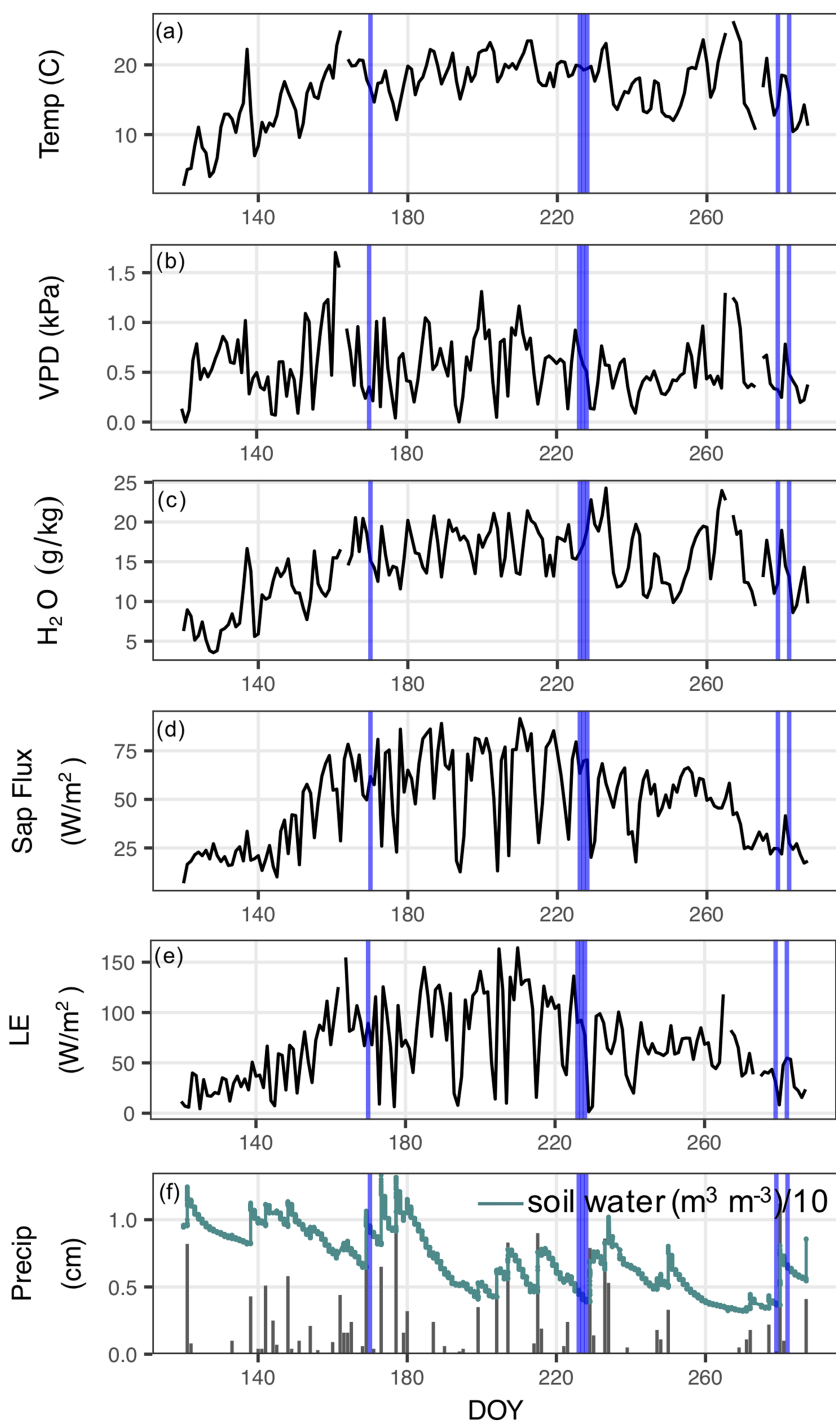


FIGURE 2 Above-canopy mean daily (a) temperature, (b) vapour pressure deficit, (c) specific humidity, (d) sap flux, (e) latent heat flux and (f) total daily precipitation and mean daily soil moisture through the growing season. The vertical blue lines indicate days on which we measured transpiration isotopes

the difference between $\delta^{18}\text{O}_x$ and $\delta^{18}\text{O}_p$ is likely related to evaporative enrichment prior to uptake (Figure 5e–h). $\delta^{18}\text{O}_s$ was never equal to $\delta^{18}\text{O}_p$, which suggests that soil water experienced fractionation by post-depositional processes (likely evaporation), was a mixture of water from multiple previous rain events and/or was fed by other nearby sources (Figure 5a–d). Near-surface soil water d -excess was lower than that of precipitation, indicating that soil water was also evaporatively enriched relative to the most recent precipitation (Figure 5e–h).

Observed $\delta^{18}\text{O}_l$ of all three species exhibited a pronounced (>10‰) daily pattern with the most evaporative enrichment (highest

$\delta^{18}\text{O}_l$ values) in the afternoon when temperature was at a maximum, relative humidity was at a minimum and sap flux was high (Figure 5a–d). As expected, d -excess of leaf water exhibited the opposite diurnal pattern with the greatest values in the morning and the lowest values in the mid-afternoon (Figure 5e–h). Observed $\delta^{18}\text{O}_l$ is generally lower than estimated steady-state $\delta^{18}\text{O}_l$, which may result from a discrepancy between observed $\delta^{18}\text{O}_l$, which includes midrib and vein water, and modelled $\delta^{18}\text{O}_l$, which estimates water at the evaporation sites. Alternatively, the offset between observed and estimated $\delta^{18}\text{O}_l$ may suggest that, even at midday when the transpiration flux was high

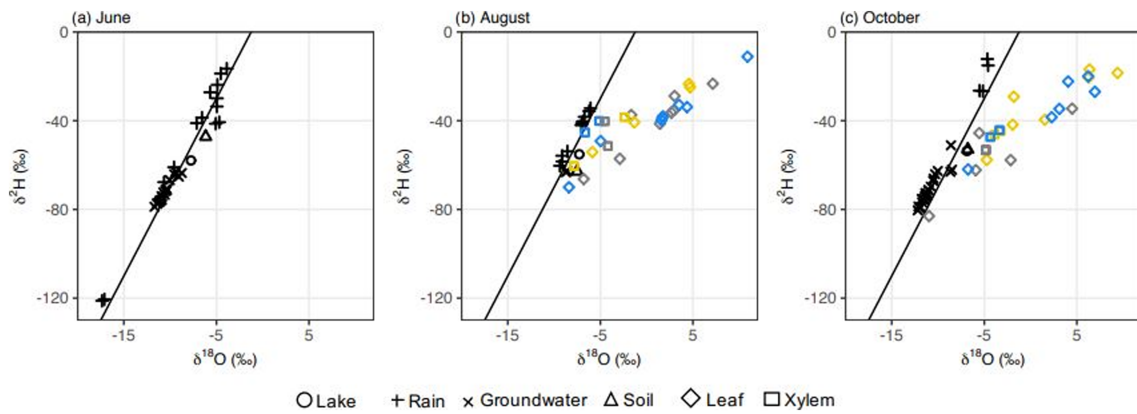


FIGURE 3 $\delta^{18}\text{O}$ and $\delta^2\text{H}$ of various waters pools at or near the study site in (a) June, (b) August, and (c) October 2017. Leaf (diamonds) and xylem (squares) isotopes are colour coded by species (maple is grey, aspen is blue, and oak is yellow). Lake, rain, ground and soil water are differentiated by symbology but are all coloured black. The black line is the global meteoric water line

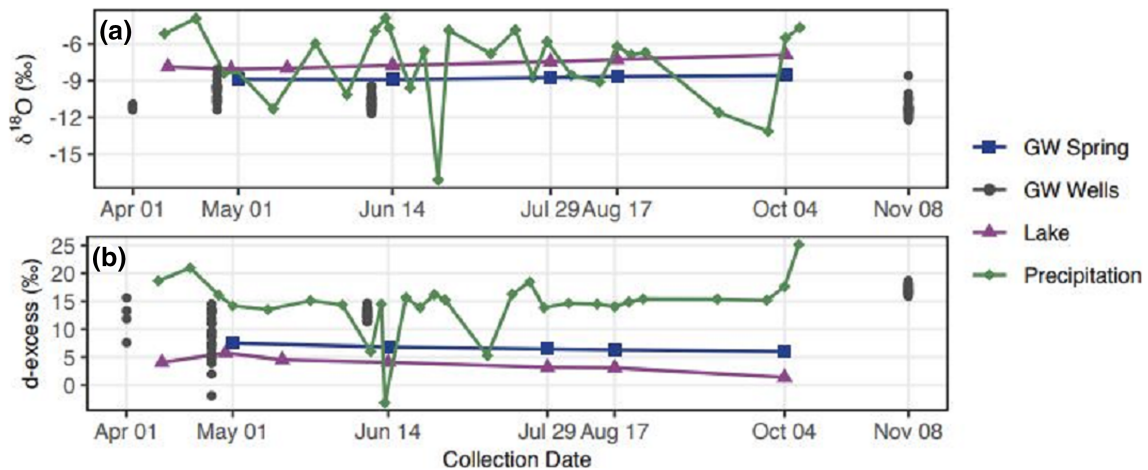


FIGURE 4 Time series of (a) $\delta^{18}\text{O}$ and (b) d -excess of precipitation (green diamond), lake (purple triangle), groundwater well (grey circle), and groundwater spring (blue square) from April to November 2017

(Figure 1a) and leaf-water turnover time was quickest, leaves were not at isotopic steady-state (Figure 5a–d).

Although the diurnal pattern of leaf water isotopes was consistent between maple, oak and aspen, the magnitude of diurnal δ_1 change and values of $\delta^{18}\text{O}_l$ and $\delta^{18}\text{O}_x$ varied between species. For example, in August morning (8 AM), $\delta^{18}\text{O}_x$ and $\delta^{18}\text{O}_l$ of oak were lower than $\delta^{18}\text{O}_x$ and $\delta^{18}\text{O}_l$ of either maple or aspen (Figure 5a). Additionally, minimum morning $\delta^{18}\text{O}_l$ varied on consecutive sampling days, with lower $\delta^{18}\text{O}_{l,\text{maple}}$ and $\delta^{18}\text{O}_{l,\text{aspen}}$ on 16 August than 15 August (Figure 5a,b). In contrast, October $\delta^{18}\text{O}_{x,\text{maple}}$, $\delta^{18}\text{O}_{x,\text{oak}}$ and $\delta^{18}\text{O}_{x,\text{aspen}}$ were within 1‰ of each other (approximately -4%), but $\delta^{18}\text{O}_{l,\text{maple}}$ was $\sim 5\%$ lower than $\delta^{18}\text{O}_{l,\text{oak}}$ and $\delta^{18}\text{O}_{l,\text{aspen}}$ (Figure 5c,d).

$\delta^{18}\text{O}_T$ varied between -15% and 6% and frequently deviated from $\delta^{18}\text{O}_x$, $\delta^{18}\text{O}_s$ or $\delta^{18}\text{O}_p$, indicating that transpiration was not at isotopic steady state on subdiurnal timescales (Figure 6). In general, $\delta^{18}\text{O}_T$ was lower in the morning when relative humidity was high and increased through the day as transpiration increased. $\delta^{18}\text{O}_T$ was always greater than $\delta^{18}\text{O}_a$ (-23.6% to -16.7% ; Figure 6) and therefore pushed the isotopic composition of atmospheric water vapour to

higher values. No consistent species-specific $\delta^{18}\text{O}_T$ trend emerged, and $\delta^{18}\text{O}_{T,\text{aspen}}$, $\delta^{18}\text{O}_{T,\text{oak}}$ and $\delta^{18}\text{O}_{T,\text{maple}}$ varied considerably day to day and on subdiurnal timescales (Figure 6). $\delta^{18}\text{O}_E$ varied between -38.3% and -31.2% and pushed $\delta^{18}\text{O}_a$ to lower values (Figure 6).

4.3 | Diurnal ET partitioning

A summary of ET partitioning results is presented in Table 2. Using Equation 3 and the measured values of $\delta^{18}\text{O}_T$, transpiration from maple, oak and aspen accounted for $37 \pm 2\%$ of the ET flux. This value, referred to as nonsteady-state F_T , did not exhibit a consistent diurnal cycle (Figure 7). We compare nonsteady-state F_T with F_T calculated from two steady-state isotope assumptions: that δ_T is equal to xylem water (source water assumption) and that δ_T is equal to δ_p of the most recent storm event (precipitation assumption). The precipitation assumption, which assumes that the only available source water is recent precipitation, allows us to estimate a transpiration flux from all species in the forest, including ones from which we did not

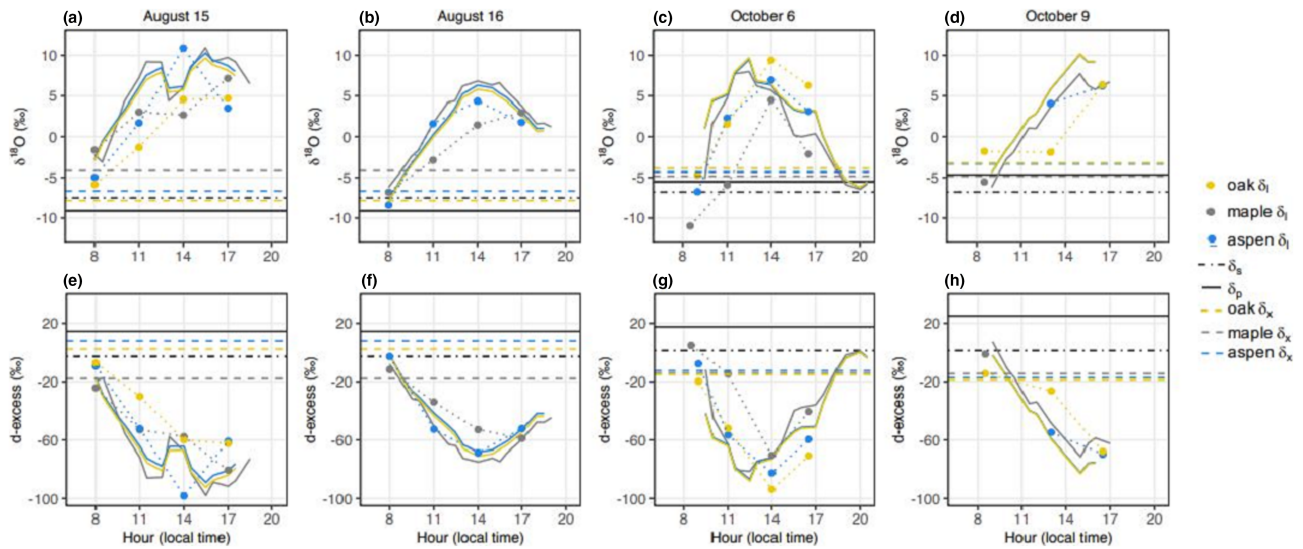


FIGURE 5 (a–d) Diurnal $\delta^{18}\text{O}$ and (e–h) d -excess of leaf water (circles), xylem (dashed lines), precipitation (solid black line) and soil water (black dotted dashed line) on (a and e) 15 August, (b and f) 16 August, (c and g) 6 October, and (d and h) 9 October. Colour differentiates species: maple is grey, aspen is blue, and oak is yellow. The solid coloured lines are expected steady state $\delta^{18}\text{O}$ and d -excess, estimated from the Craig and Gordon (1965) using values of the kinetic fractionation factor from Merlivat (1978). Values of δ_x on 15 August are assumed to be the same as those measured on 16 August

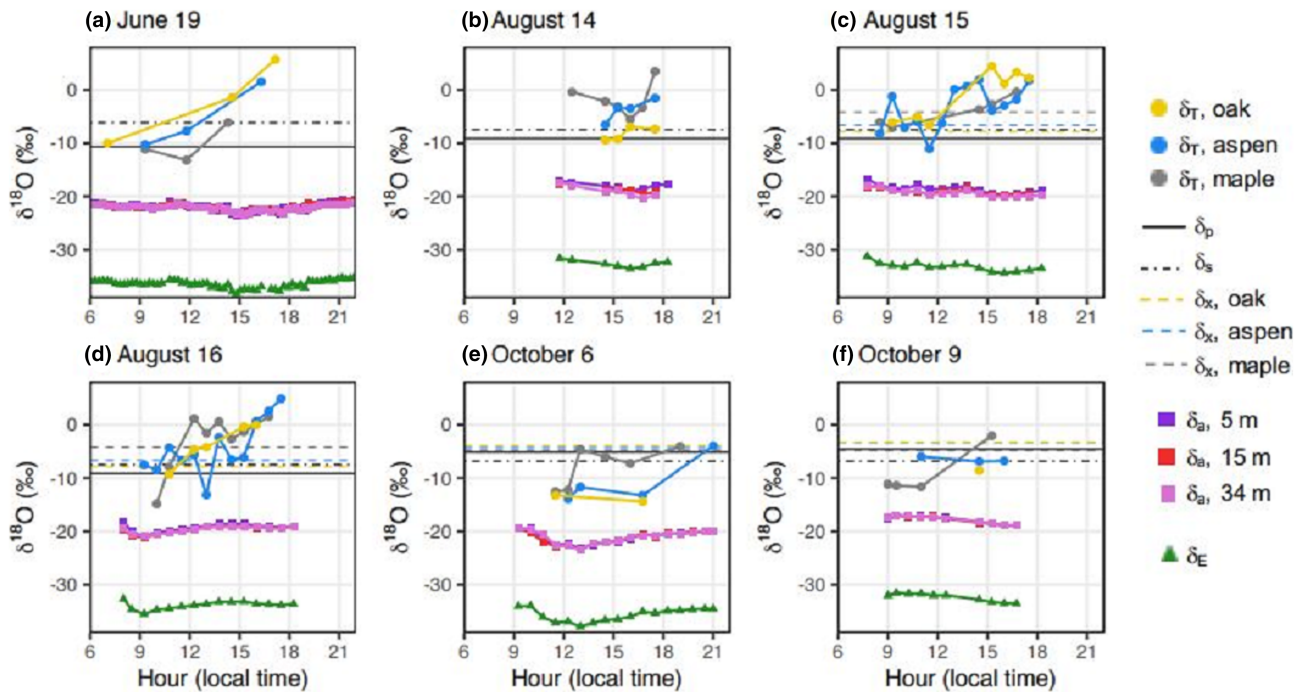


FIGURE 6 Diurnal δ_T (circles), δ_a (squares) and δ_E (triangles) on six days of measurements. For δ_T , maple is grey, aspen is blue, and oak is yellow. For δ_a , 5 m is purple, 15 m is red, and 34 m is pink. Horizontal lines indicate δ_p (solid black) of recent precipitation, δ_s (dotted dash black) and δ_x (dashed, maple is yellow, aspen is blue, and oak is grey)

measure δ_x . The precipitation assumption is our best attempt to quantitatively estimate a plot-level transpiration flux; it does not address the timescale over which plants access available soil water or the complexities of preferential flow paths through soils, both of which affect δ_x and δ_T (Allen, Kirchner, & Goldsmith, 2018; Brooks et al., 2010; Evaristo, Jasechko, & McDonnell, 2015).

F_T estimated from the source water assumption ($36 \pm 2\%$, Figure 7) is nearly identical to nonsteady-state F_T . The precipitation assumption produces a higher estimate of F_T ($53 \pm 3\%$, Figure 7). The offset between these F_T values arises because the precipitation assumption includes a water flux from all tree species at the site while the source water assumption only includes the species from which we

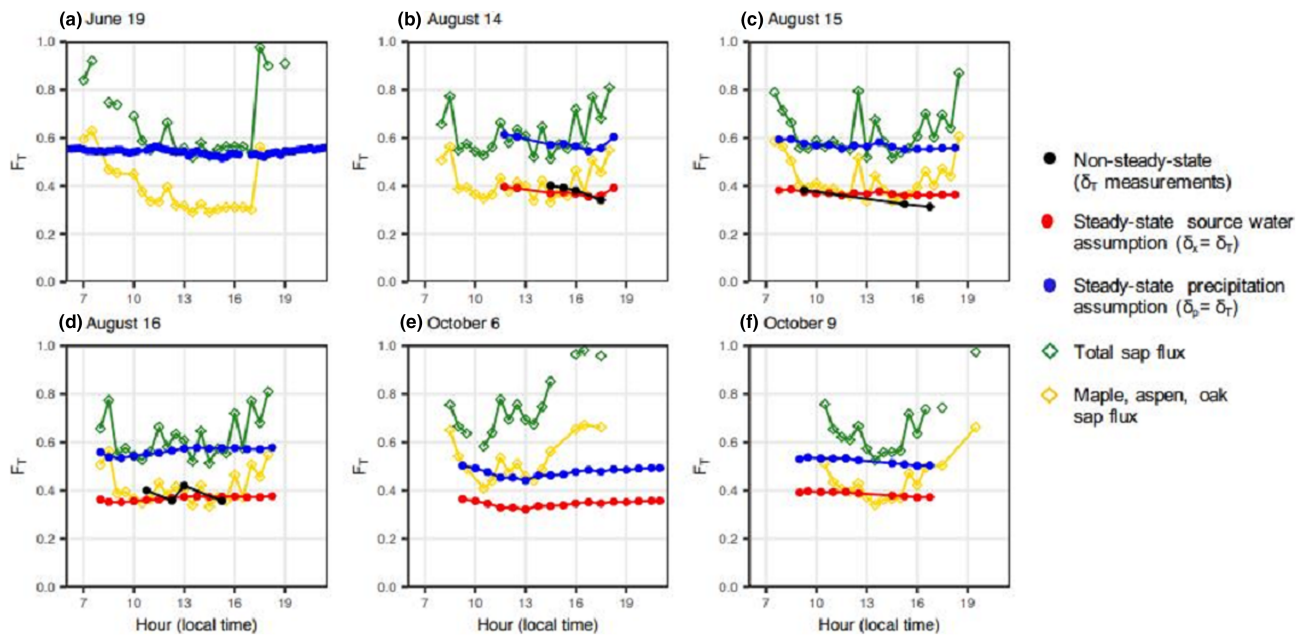


FIGURE 7 Isotopic (filled circles) and ecohydrologic (open diamonds) F_T on six days of measurements. F_T estimated with nonsteady-state measurements (black), the source water assumption (red) and sap flux scaled to include only medium maple, large oak and large aspen (yellow) only capture the transpiration flux from a subset of trees. F_T from the precipitation assumption (blue) and plot-level sap flux (green) capture the transpiration flux from all species and size classes in the forest

measured δ_x (maple, oak and aspen) and accounts for $\sim 70\%$ of the site LAI. Correcting for this LAI discrepancy (scaling F_T results from the precipitation assumption to include only 70% of the trees) and assuming that each species produces a similar amount of transpiration per unit leaf (Jarvis & McNaughton, 1986), we find that the source water assumption (36%) and the precipitation assumption (37%) produce nearly identical estimates of F_T . Agreement between the two steady-state δ_T assumptions suggests that at this site either technique is a precise approach to measuring forest F_T . The plot-level F_T results ($53 \pm 3\%$) agree with other estimates of forest F_T (Berkelhammer et al., 2016; Matheny, Bohrer, Vogel, et al., 2014; Sun et al., 2014; Tsujimura et al., 2007; Zhou, Yu, Zhang, Huang, & Wang, 2016). Like nonsteady-state F_T , F_T calculated using the either source water or precipitation assumptions exhibits no diurnal variation (Figure 7).

Finally, we compare isotopic ET partitioning results with F_T estimated using eddy covariance and sap flux data (Figure 7). The sap flux network at this site is extensive and, coupled with eddy covariance data, provides a wide range of information about forest water fluxes including an estimate of F_T . For simplicity, we refer to F_T calculated using eddy covariance and sap flux data as the ecohydrologic ET partitioning technique. Plot-level ecohydrologic F_T was $65 \pm 12\%$; ecohydrologic F_T scaled to include only the transpiration flux from maple, oak and aspen was $43 \pm 9\%$ (Figure 7). Agreement between the isotopic and ecohydrologic partitioning techniques was stronger midday (10 AM to 4 PM, $61 \pm 8\%$ plot-level F_T ; $40 \pm 7\%$ F_T for maple, oak and aspen) when water fluxes were high and weaker in the morning and evening when water fluxes were lower. When F_T from the isotopic and ecohydrologic ET partitioning techniques diverged, the ecohydrologic partitioning technique tended to estimate higher F_T

than the isotopic technique (Figure 7). Neither partitioning approach revealed a consistent nor pronounced daytime F_T cycle.

5 | DISCUSSION

5.1 | Isotope data as an indicator of local hydrology

5.1.1 | Observations of nonsteady-state δ_T

It has long been recognized that on timescales longer than the plant-water turnover time, the isotopic composition of vapour that is transpired from a leaf must equal the water that enters the leaf from the source (Dongmann, Nürnberg, Forstel, & Wagener, 1974). Accordingly, most isotope models assume that transpiration is a non-fractionating process, at least on longer timescales (Farquhar & Cernusak, 2005; Flanagan et al., 1991; Haese et al., 2013; Wang & Yakir, 1995). However, on short timescales (subdiurnal to a few days), recent observations have revealed that δ_T deviates from steady-state conditions because environmental conditions change quicker than the turnover of plant water (Dubbert et al., 2017; Dubbert, Piayda, et al., 2014; Harwood, Gillon, Griffiths, & Broadmeadow, 1998; Simonin et al., 2013; Wang & Yakir, 1995; Yakir, Berry, Giles, & Osmond, 1994). δ_T varies with abiotic and biotic conditions including stomatal conductance, temperature, humidity and δ_a (Simonin et al., 2013). At the leaf level, δ_T is also controlled by the transpiration rate, stomatal density and leaf water content (Buckley, 2019; Dubbert et al., 2017). The Craig and Gordon (1965) model predicts that temperature and humidity are correlated with δ_T (Dongmann et al., 1974; Farquhar et al., 1993;

Farquhar & Cernusak, 2005; Farquhar & Lloyd, 1993; Farris & Strain, 1978; Flanagan et al., 1991), which Simonin et al. (2013) confirmed in a leaf-cuvette study, and we find to be true in naturally varying conditions (Figure 6).

We measured δ_T from three broadleaf deciduous trees but did not find consistent species-specific δ_T patterns (Figure 6). In contrast, in a controlled greenhouse, Dubbert et al. (2017) measured δ_T from a variety of herbs, shrubs and trees and linked δ_T variations to species-specific differences in the transpiration rate, stomatal aperture, stomatal density and leaf water content. At our field site, oak has an extensive rooting structure and can access a deeper, isotopically more depleted soil water pool than maple, which are shallow rooting (Matheny et al., 2017), although these uptake dynamics may be site-specific (Lanning, Wang, Benson, Zhang, & Novick, 2020). We therefore expected that the isotopic composition of xylem, leaf and transpired water from oaks would be less than that from maples and aspen, but this was only true of xylem and leaf water in August when soil moisture was low. Rain storms on 4 October and 7 October moistened the soil and provided near-surface moisture for the maple, oak and aspen trees to transpire. When the soil was drier during the August sampling period, the oak favoured a more abundant, deeper isotopically more negative water source (Matheny et al., 2017). Taken together, these results suggest that when broadleaf deciduous trees are not water stressed, species-specific effects on local isotope signals are difficult to identify and distinguish. In contrast, when these trees are water stressed, species-specific differences may be evident in water isotope signals.

5.1.2 | Surface, terrestrial and biologic water isotope variability

The isotopic composition of precipitation at UMBS reflects the dominant fractionation processes in northern Michigan, Rayleigh distillation and 'lake-effect' precipitation (Bowen et al., 2012). Previous estimates suggest that up to 32% of precipitation in this region is derived from evaporation over Lake Michigan (Bowen et al., 2012; Gat, Bowser, & Kendall, 1994; Machavaram & Krishnamurthy, 1995). This high degree of moisture recycling explains the high ($\sim 13\%$) observed precipitation d -excess. The seasonal increase (decrease) of $\delta^{18}\text{O}_{\text{lake}}$ (d -excess $_{\text{lake}}$) indicates that evaporation of local surface water likely also added vapour with a high d -excess to the atmosphere (Figure 4).

The dome-shaped pattern of diurnal δ_l has been observed in many studies and is related to the changes in VPD and transpiration rate (Cernusak et al., 2016 and references therein). Among the broadleaf deciduous trees in this study, the shape and magnitude of the diurnal $\delta^{18}\text{O}_l$ pattern were independent of species type and were broadly consistent with common isotopic leaf water models (Farquhar & Cernusak, 2005). The initial, morning isotopic composition of $\delta^{18}\text{O}_l$ did, however, vary between the three species and was particularly notable on 16 August ($\delta^{18}\text{O}_{l,\text{oak}}$, Figure 5b,e) and 6 October ($\delta^{18}\text{O}_{l,\text{maple}}$, Figure 5c,f). These differences may be related to rooting strategy when the soils are dry (Matheny et al., 2017) or may arise

due to the high sand content and low moisture retention of soils that can cause high spatial variability of δ_s or δ_x at the site (He et al., 2013; Nave et al., 2011).

5.2 | ET partitioning

ET partitioning distinguishes the evaporation and transpiration components of the ET flux and helps provide a quantitative understanding of ecological processes within the water cycle (Jasechko et al., 2013; Kool et al., 2014). Isotopic ET partitioning is predicated on E and T fluxes of distinct isotopic compositions and accurate estimates of δ_{ET} , δ_E and δ_T . Currently, there is no consensus on the best approach to measure the isotopic composition of the ET flux, and researchers use either Keeling mixing models or the flux-gradient technique (Good, Soderberg, Wang, & Caylor, 2012). The flux-gradient method works best over smooth, homogenous surfaces such as lakes and grasses (Xiao et al., 2017); we chose the Keeling approach to avoid complications of canopy turbulence that may limit the flux-gradient method (Good et al., 2012; Yakir & Wang, 1996). Other ET partitioning studies (e.g., Berkelhammer et al., 2016; Sun et al., 2014; Tsujimura et al., 2007) have also successfully used the Keeling method to calculate δ_{ET} in forested environments, which further justifies our approach to estimating δ_{ET} .

We used the Craig and Gordon (1965) model (Equation 5) to calculate δ_E . Here, the challenging factors are an accurate and representative value for the isotopic composition of soil water at the evaporation front and the soil kinetic fractionation factor (Wang et al., 2013; Xiao et al., 2018). We collected soil from the top 10 cm and used δ_s from a single location to estimate the evaporative flux over the entire tower footprint. This approach does not capture the spatial heterogeneity of δ_s (Gazis & Feng, 2004; Hsieh, Chadwick, Kelly, & Savin, 1998) but is a common approach in most ET partitioning studies (e.g., Aouade et al., 2016; Dubbert, Cuntz, et al., 2014; Yopez et al., 2005; Zhang, Shen, Sun, & Gates, 2011). The closed, thick canopy cover at our field site (Aron et al., 2019) likely reduces spatial variation in δ_s . The kinetic fractionation factor in soil evaporation studies has long been a point of debate and varies with soil tortuosity, soil moisture and atmospheric conditions (Quade, Brüggemann, Graf, Vereecken, & Rothfuss, 2018; Xiao et al., 2018). In our study, diurnal soil water content was relatively consistent (varied by less than 0.5% [$\text{m}^3 \text{m}^{-3}$] per day), so we elected to use the constant value for ϵ_k provided by Quade et al. (2018).

Most isotope-based ET studies assume transpiration is in isotopic-steady state and estimate that δ_T is equal to δ_x or δ_s (e.g., Aouade et al., 2016; Wang & Yakir, 2000; Yopez, Williams, Scott, & Lin, 2003; Zhang et al., 2011). Instead, in this study, we measured δ_T using a leaf chamber to (1) observe any nonsteady-state transpiration isotope patterns and (2) evaluate whether direct δ_T measurements affect isotopic ET partitioning. The technical and methodological advancements for this type of measurement have only recently been developed (e.g., Wang et al., 2012), and to date, only a handful of studies have used a leaf chamber to measure δ_T and

partition F_T (Dubbert, Cuntz, et al., 2014; Good et al., 2014; Lu et al., 2017; Wang et al., 2010, 2013; Wu et al., 2017). However, nearly all of this work has been done in agricultural fields or grasslands, and still relatively little is known about δ_T (Lanning et al., 2020) and isotope-inferred F_T in forests.

The daytime, plot-level values of F_T reported in this study (53% from the precipitation assumption; 61% from the ecohydrologic technique, Figure 7) agree well with other estimates of forest F_T . Berkelhammer et al. (2016) and Tsujimura et al. (2007) used water isotopes to calculate forest F_T values of 49%–62% and 60%–73%, respectively. Non-isotope ET partitioning techniques reveal similar F_T and range from 52% (Zhou et al., 2016) to ~70%–80% (Matheny, Bohrer, Vogel, et al., 2014; Sulman, Roman, Scanlon, Wang, & Novick, 2016) in deciduous broadleaf forest sites. At our field site, Matheny, Bohrer, Vogel, et al. (2014) and Aron et al. (2019) demonstrated that ET partitioning is sensitive to forest structure and LAI, with a greater transpiration flux from closed forest canopies and a greater evaporation flux from open forest canopies. The positive relationship between LAI and F_T is also observed in a variety of nonforest environments (Scott & Biederman, 2017; Wang, Good, & Caylor, 2014; Wei et al., 2017), although it is poorly parameterized in most LSMs, with estimates of F_T that are typically lower than expected (Bowen et al., 2019).

In this study, midday F_T did not exhibit a consistent cycle regardless of species, steady-state assumption or partitioning technique (Figure 7). Because LAI sets F_T , Wang et al. (2014) proposed that F_T should be relatively consistent throughout the growing season. Although F_T can vary with passing weather systems and precipitation (e.g., Aron et al., 2019; Wen, Yang, Sun, & Lee, 2016), periods of water stress (Good et al., 2014; Matheny et al., 2017) and the removal of biomass (e.g., harvesting or cutting grass) (Wang, Yamanaka, Li, & Wei, 2015), Berkelhammer et al. (2016) demonstrated that forest F_T was generally invariant on seasonal timescales. We come to the same conclusions on subdiurnal timescales (Figure 7), although this observation may be dependent on vegetation type, aridity and soil moisture. For example, in arid sites with very low soil moisture, diurnal increases in the transpiration flux may not be accompanied by a concurrent evaporation flux, and F_T may increase midday (Zhou, Yu, Zhang, Huang, & Wang, 2018). However, the absence of a diurnal F_T cycle at our broadleaf deciduous forest site suggests that similar ecological processes and environmental conditions drive the component ET fluxes in this environment as both evaporation and transpiration fluxes are controlled by external environmental factors including VPD, incoming solar radiation, temperature, humidity, wind speed, water availability and ambient CO_2 concentration as well as a number of internal soil or plant factors (e.g., tortuosity, available surface area and water potential) (Ball, 1988; Cernusak et al., 2016; Penman, 1948; Sperry, Hacke, Oren, & Comstock, 2002; Tyree & Zimmerman, 2002).

Finally, we compare F_T from the isotopic and ecohydrologic partitioning techniques. Isotopic and ecohydrologic derived F_T was similar during the day when ET was high, but results from the two techniques diverged in the early morning and late afternoon when water fluxes were lower. The timing of diurnal sap flux is usually well

correlated with incoming solar radiation, temperature and VPD (Ling et al., 2008). It is therefore possible that the high ecohydrologic F_T in the morning and evening reflects differences in the initiation and termination of early morning and late afternoon diurnal evaporation and transpiration fluxes. However, both steady-state isotopic F_T estimates remained invariant during these times (field logistics and low water fluxes prohibited direct δ_T measurements in the early morning and evening), suggesting that the high morning and afternoon ecohydrologic F_T may be an artefact of sap flux or eddy covariance measurements. To this point, sap flux measurements are known to be biased and prone to errors when water fluxes are low (Ewers & Oren, 2000; Granier, 1987). High ecohydrologic F_T may also be explained by the refilling of dehydrated xylem tissues that does not necessarily result in the release of water to the atmosphere at that time. The midday agreement between isotopic nonsteady-state, isotopic steady-state and ecohydrologic partitioning techniques highlights the precision of these different approaches. Despite a multitude of assumptions and simplifications, these techniques capture the same water fluxes that are driven by incoming solar radiation, water availability and plant hydraulics. Additional ET partitioning techniques such as solar-induced fluorescence (SIF) (Lu et al., 2018; Shan et al., 2019) may soon be available at this site and may yield new insights into the divergent partitioning results in the early morning and late afternoon.

5.3 | Caveats and experimental considerations

Forests play a critical role in the water cycle and imprint a distinct signature on the isotopic composition of local and regional water cycles. However, measuring forest water fluxes is difficult because forests are heterogeneous, turbulent environments. Accordingly, studies of forest δ_T (e.g., Lanning et al., 2020) and isotopic ET partitioning have lagged behind similar studies in greenhouses or homogenous environments such as croplands and grasslands (e.g., Dubbert et al., 2017; Good et al., 2014). While our experimental approach mitigates this gap, this study was affected by field logistics. For example, we were only able to reach three trees for transpiration measurements. As a result, F_T from δ_T measurements, the source water assumption and sap flux scaled to include only the transpiration flux from maples, oaks and aspen are biased low.

Limitations of the experimental set-up are also an important consideration. First, direct δ_T calculations require that a leaf be manually inserted and removed from a sampling chamber, which limits the number of measurements. We likely missed water fluxes before and after our measurement periods. Second, the different measurement heights (5 m for maple, 15 m for aspen and oak) may complicate species-specific observations of δ_T . Although vertical light-induced differences in stomatal conductance and leaf temperature can balance each other (Bögelein, Thomas, & Kahmen, 2017), even small differences in measurement location and microclimate within the canopy can strongly affect transpiration and δ_T (Baldocchi, Wilson, & Gu, 2002; Chen et al., 1999; Jarvis & McNaughton, 1986). Third, scaling isotopic ET partitioning from local measurements to a plot or regional scale

remains a challenge given soil heterogeneity, diversity of plant eco-physiology and a variety of vegetative and canopy structures. Sap flux measurements suffer from similar scaling challenges (Schaeffer, Williams, & Goodrich, 2000); however, our field site has an unusually robust sap flux network that has been successfully statistically scaled to plot-level water fluxes (Matheny, Bohrer, Vogel, et al., 2014). Scaling individual soil and tree isotope measurements to the plot-level remains difficult (Sutanto et al., 2014).

5.4 | Implications and directions of future work

Moving forward, we show that continuous analysis of δ_a and routine measurements of δ_x or δ_p can efficiently record F_T . Researchers should make measurements for the source water (δ_x) or precipitation (δ_p) approaches based on site-specific characteristics such as species distribution, expected δ_s heterogeneity and the frequency of precipitation events. Neither approach requires laborious leaf chamber measurements, and both are founded on a steady-state assumption about δ_T that is valid for midday (Figure 7) and seasonal (e.g., Wei et al., 2015) isotopic ET partitioning. In contrast, assumptions of steady-state δ_T may not suffice for questions related to isotope and water cycles on subdiurnal timescales (e.g., Aron et al., 2019; Simonin et al., 2013; Welp et al., 2012). On this relatively short timescale, nonsteady-state δ_T measurements inform how transpiration forces the isotopic composition of atmospheric water vapour and may help validate the Craig and Gordon (1965) model that is commonly used to estimate δ_T and δ_E (e.g., Dubbert et al., 2013; Dubbert et al., 2014; Good et al., 2012; Hu et al., 2014). Additionally, studies that measure and model δ_T can partition species-specific F_T to learn about species-specific hydrology and responses to environmental conditions. Observation of δ_T may also improve the parameterization of kinetic isotope effects during evaporation and transpiration, which remains a major challenge in isotope ecohydrology research (Quade et al., 2018).

Overall, continued efforts to accurately measure and understand local transpiration are critical to expand our knowledge of continental water recycling and understand the role that plants play in regulating water budgets. This study examines forest ET fluxes; additional observations from environments such as wetlands and tundra are still needed to assess how hydrologic processes are represented in LSMs and to monitor how water and energy fluxes respond to climate and land use change. Currently, almost all LSMs underestimate F_T . Recent and ongoing efforts to incorporate water isotopes into LSMs (e.g., Wong et al., 2017) may improve our understanding of land-atmosphere water fluxes, but these models must be validated with measurements of local δ_T and F_T .

6 | CONCLUSIONS

We present direct, species-specific measurements of $\delta^{18}\text{O}_T$ from three broadleaf deciduous trees and estimate the contribution of transpiration to the ET flux in a mixed deciduous forest. The

methodology to make δ_T measurements in a field setting is new, and these are among the first δ_T results obtained from a forest environment. $\delta^{18}\text{O}_T$ deviated from isotopic steady-state on sub-diurnal timescales but did not exhibit a clear species-specific pattern. Using water isotopes, we found that the F_T was invariant during the day, which indicates that similar atmospheric and micrometeorologic conditions control evaporation and transpiration fluxes at this site. We find strong midday agreement between isotopic steady-state, isotopic nonsteady-state and ecohydrologic (eddy covariance and sap flux) estimates of F_T , which suggests that assumptions of steady-state δ_T may suffice for other forest ET partitioning studies. Agreement between the isotopic and ecohydrologic partitioning techniques, in particular the absence of a diurnal cycle using either approach, should encourage use of the isotopic ET partitioning method in environments where it is impossible or logistically impractical to install sap flux sensors. Transpiration and ET remain challenging fluxes to measure, model and predict, but water isotopes can help improve our understanding of these important hydrological processes. Future work on nonsteady-state δ_T will improve the utility water vapour isotopes as a tool to study land-atmosphere water exchange, while steady-state assumptions of δ_T and isotopic ET partitioning can provide insight into the role of plants in terrestrial water cycling.

ACKNOWLEDGEMENTS

We thank Chris Vogel for assistance running the isotope analysers, Luke Nave and Katy Hofmeister for collecting groundwater samples, and Molly Cavaleri and Evan Kane for assistance designing the cryodistillation apparatus. We thank two anonymous reviewers for comments and suggestions that improved this manuscript.

CONFLICT OF INTEREST

The authors declare no conflicts of interest.

DATA AVAILABILITY STATEMENT

Data associated with this study are archived and freely available from the University of Michigan Biological Station Data Repository (<http://biostation.lsa.umich.edu/data>).

FUNDING INFORMATION

Funding for AmeriFlux data resources was provided by the U.S. Department of Energy's Office of Science. Funding for this study was provided by U.S. Department of Energy's Office of Science, Office of Biological and Environmental Research, Terrestrial Ecosystem Sciences Program award DE-SC0007041 and the AmeriFlux Management program under Flux Core Site agreement 7096915 through Lawrence Berkeley National Laboratory. P.G.A. received funding from the University of Michigan Department of Earth and Environmental Sciences, University of Michigan Rackham Graduate School and the University of Michigan Biological Station. C.J.P. received funding from NSF Tectonics Program award 1550101. R.P.F. received funding from NSF Macrosystems Biology Early Neon

Science award 1802880. A.M.M received funding from NSF Hydrological Science grant 1521238.

ORCID

Phoebe G. Aron  <https://orcid.org/0000-0002-4700-5445>

Christopher J. Poulsen  <https://orcid.org/0000-0001-5104-4271>

Richard P. Fiorella  <https://orcid.org/0000-0002-0824-4777>

Ashley M. Matheny  <https://orcid.org/0000-0002-9532-7131>

REFERENCES

- Aemisegger, F., Sturm, P., Graf, P., Sodemann, H., Pfahl, S., Knohl, A., & Wernli, H. (2012). Measuring variations of $\delta^{18}\text{O}$ and $\delta^2\text{H}$ in atmospheric water vapour using two commercial laser-based spectrometers: An instrument characterisation study. *Atmospheric Measurement Techniques*, 5, 1491–1511. <https://doi.org/10.5194/amt-5-1491-2012>
- Allen, S. T., Kirchner, J. W., & Goldsmith, G. R. (2018). Predicting spatial patterns in precipitation isotope ($\delta^2\text{H}$ and $\delta^{18}\text{O}$) seasonality using sinusoidal isoscapes. *Geophysical Research Letters*, 45(10), 4859–4868. <https://doi.org/10.1029/2018GL077458>
- Anderegg, W. R. L., Trugman, A. T., Bowling, D. R., Salvucci, G., & Tuttle, S. E. (2019). Plant functional traits and climate influence drought intensification and land-atmosphere feedbacks. *Proceedings of the National Academy of Sciences*, 116(28), 14071–14076. <https://doi.org/10.1073/pnas.1904747116>
- Aouade, G., Ezzahar, J., Amenzou, N., Er-raki, S., Benkaddour, A., & Khabba, S. (2016). Combining stable isotopes, eddy covariance system and meteorological measurements for partitioning evapotranspiration, of winter wheat, into soil evaporation and plant transpiration in a semi-arid region. *Agricultural Water Management*, 177, 181–192. <https://doi.org/10.1016/j.agwat.2016.07.021>
- Aron, P. G., Poulsen, C. J., Fiorella, R. P., & Matheny, A. M. (2019). Stable water isotopes reveal effects of intermediate disturbance and canopy structure on forest water cycling. *Journal of Geophysical Research – Biogeosciences*, 124, 2958–2975. <https://doi.org/10.1029/2019JG005118>
- Badgley, G., Fisher, J. B., Jimenez, C., Tu, K. P., & Vinukollu, R. (2015). On uncertainty in global terrestrial evapotranspiration estimates from choice of input forcing datasets. *Journal of Hydrometeorology*, 16, 1449–1455. <https://doi.org/10.1175/JHM-D-14-0040.1>
- Bailey, A., Noone, D., Berkelhammer, M., Steen-Larsen, H. C., & Sato, P. (2015). The stability and calibration of water vapor isotope ratio measurements during long-term deployments. *Atmospheric Measurement Techniques*, 8(10), 4521–4538. <https://doi.org/10.5194/amt-8-4521-2015>
- Baldocchi, D. D., Wilson, K. B., & Gu, L. (2002). How the environment, canopy structure and canopy physiological functioning influence carbon, water and energy fluxes of a temperate broad-leaved deciduous forest—An assessment with the biophysical model CANOAK. *Tree Physiology*, 22(15–16), 1065–1077. <https://doi.org/10.1093/treephys/22.15-16.1065>
- Ball, J. T. (1988). *An analysis of stomatal conductance*. Thesis (Ph. D.), Stanford University.
- Barbour, M. M. (2007). Review: Stable oxygen isotope composition of plant tissue. *Functional Plant Biology*, 34, 83–94. <https://doi.org/10.1071/FP06228>
- Berkelhammer, M., Noone, D. C., Wong, T. E., Burns, S. P., Knowles, J. F., Kaushik, A., ... Williams, M. W. (2016). Convergent approaches to determine an ecosystem's transpiration fraction. *Global Biogeochemical Cycles*, 30(6), 933–951. <https://doi.org/10.1002/2016GB005392>
- Bögelein, R., Thomas, F. M., & Kahmen, A. (2017). Leaf water ^{18}O and ^2H enrichment along vertical canopy profiles in a broadleaved and a conifer forest tree. *Plant, Cell and Environment*, 40, 1086–1103. <https://doi.org/10.1111/pce.12895>
- Bowen, G. J., Cai, Z., Fiorella, R. P., & Putman, A. L. (2019). Isotopes in the water cycle: Regional- to global-scale patterns and applications. *Annual Reviews*, 47, 453–479. <https://doi.org/10.1146/annurev-earth-053018-060220>
- Bowen, G. J., Kennedy, C. D., Henne, P. D., & Zhang, T. (2012). Footprint of recycled water subsidies downwind of Lake Michigan. *Ecosphere*, 3(6), 1–16. <https://doi.org/10.1890/ES12-00062.1>
- Brooks, J. R., Barnard, H. R., Coulombe, R., & McDonnell, J. J. (2010). Ecohydrologic separation of water between trees and streams in a Mediterranean climate. *Nature Geoscience*, 3, 100–104. <https://doi.org/10.1038/NGEO722>
- Brutsaert, W. (2017). Advances in water resources global land surface evaporation trend during the past half century: Corroboration by Clausius-Clapeyron scaling. *Advances in Water Resources*, 106, 3–5. <https://doi.org/10.1016/j.advwatres.2016.08.014>
- Buckley, T. N. (2019). How do stomata respond to water status? *New Phytologist*, 224, 21–36. <https://doi.org/10.1111/nph.15899>
- Cernusak, L. A., Barbour, M. M., Arndt, S. K., Cheesman, A. W., English, N. B., Feild, T. S., ... Farquhar, G. D. (2016). Stable isotopes in leaf water of terrestrial plants. *Plant, Cell & Environment*, 39(5), 1087–1102. <https://doi.org/10.1111/pce.12703>
- Chang, L., Dwivedi, R., Knowles, J. F., Fang, Y., Niu, G.-Y., Pelletier, J. D., ... Meixner, T. (2018). Why do large-scale land surface models produce a low ratio of transpiration to evapotranspiration? *Journal of Geophysical Research-Atmospheres*, 123, 9109–9130. <https://doi.org/10.1029/2018JD029159>
- Chen, J., Saunders, S. C., Crow, T. R., Naiman, R. J., Kimberley, D., Mroz, G. D., ... Franklin, J. F. (1999). Microclimate in forest ecosystem and landscape ecology. *Bioscience*, 49(4), 288–297. <https://doi.org/10.2307/1313612>
- Coplen, T. B. (1996). New guidelines for reporting stable hydrogen, carbon, and oxygen isotope-ratio data. *Geochimica et Cosmochimica Acta*, 60(17), 3359–3360. [https://doi.org/10.1016/0016-7037\(96\)00263-3](https://doi.org/10.1016/0016-7037(96)00263-3)
- Craig, H. (1961). Isotopic variations in meteoric waters. *Science*, 133(3465), 1702–1703. <https://doi.org/10.1126/science.133.3465.1702>
- Craig, H., & Gordon, L. I. (1965). Deuterium and oxygen-18 variations in the ocean and the marine atmosphere. In E. Tongiorgi (Ed.), *Proceedings of a conference on stable isotopes in oceanographic studies and paleotemperatures* (pp. 9–130). Pisa, Italy: Laboratory of Geology and Nuclear Science.
- Dansgaard, W. (1964). Stable isotopes in precipitation. *Tellus*, 16(4), 436–468. <https://doi.org/10.3402/tellusa.v16i4.8993>
- De Kauwe, M. G., Medlyn, B. E., Knauer, J., & Williams, C. A. (2017). Ideas and perspectives: How coupled is the vegetation to the boundary layer? *Biogeosciences*, 14, 4435–4453. <https://doi.org/10.5194/bg-14-4435-2017>
- Dongmann, G., Nürnberg, H. W., Forstel, H., & Wagoner, K. (1974). On the enrichment of H_2^{18}O in the leaves of transpiring plants. *Radiation and Environmental Biophysics*, 11, 41–52. <https://doi.org/10.1007/BF01323099>
- Dubbert, M., Cuntz, M., Piayda, A., Maguás, C., & Werner, C. (2013). Partitioning evapotranspiration—Testing the Craig and Gordon model with field measurements of oxygen isotope ratios of evaporative fluxes. *Journal of Hydrology*, 496, 142–153. <https://doi.org/10.1016/j.jhydrol.2013.05.033>
- Dubbert, M., Cuntz, M., Piayda, A., & Werner, C. (2014). Oxygen isotope signatures of transpired water vapor: The role of isotopic non-steady-state transpiration under natural conditions. *New Phytologist*, 203, 1242–1252. <https://doi.org/10.1111/nph.12878>
- Dubbert, M., Kübert, A., & Werner, C. (2017). Impact of leaf traits on temporal dynamics of transpired oxygen isotope signatures and its impact on atmospheric vapor. *Frontiers in Plant Science*, 8(January), 1–12. <https://doi.org/10.3389/fpls.2017.00005>

- Dubbert, M., Piayda, A., Cuntz, M., Correia, A. C., Silva, F. C. e., Pereira, J. S., & Werner, C. (2014). Stable oxygen isotope and flux partitioning demonstrates understory of an oak savanna contributes up to half of ecosystem carbon and water exchange. *Frontiers in Plant Science*, 5, 1–16. <https://doi.org/10.3389/fpls.2014.00530>
- Dunn, S. M., & Mackay, R. (1995). Spatial variation in evapotranspiration and the influence of land use on catchment hydrology. *Journal of Hydrology*, 171, 49–73. [https://doi.org/10.1016/0022-1694\(95\)02733-6](https://doi.org/10.1016/0022-1694(95)02733-6)
- Ehleringer, J. R., & Dawson, T. E. (1992). Water uptake by plants: Perspectives from stable isotope composition. *Plant, Cell and Environment*, 15, 1073–1082. <https://doi.org/10.1111/j.1365-3040.1992.tb01657.x>
- Ellison, D., Morris, C. E., Locatelli, B., Sheil, D., Cohen, J., Murdiyarsa, D., ... Sullivan, C. A. (2017). Trees, forests and water: Cool insights for a hot world. *Global Environmental Change*, 43, 51–61. <https://doi.org/10.1016/j.gloenvcha.2017.01.002>
- Evaristo, J., Jasechko, S., & McDonnell, J. J. (2015). Global separation of plant transpiration from groundwater and streamflow. *Nature*, 525, 91–94. <https://doi.org/10.1038/nature14983>
- Ewers, B. E., & Oren, R. A. M. (2000). Analyses of assumptions and errors in the calculation of stomatal conductance from sap flux measurements. *Tree Physiology*, 20, 579–589. <https://doi.org/10.1093/treephys/20.9.579>
- Fang, Y., Leung, L. R., Duan, Z., Wigmosta, M. S., Maxwell, R. M., Chambers, J. Q., & Tomasella, J. (2017). Influence of landscape heterogeneity on water available to tropical forests in an Amazonian catchment and implications for modeling drought response. *Journal of Geophysical Research-Atmospheres*, 122, 8410–8426. <https://doi.org/10.1002/2017JD027066>
- Farquhar, G. D., & Cernusak, L. A. (2005). On the isotopic composition of leaf water in the non-steady state. *Functional Plant Biology*, 32(1974), 293–303. <https://doi.org/10.1071/FP04232>
- Farquhar, G. D., & Lloyd, J. (1993). Carbon and oxygen isotope effects in the exchange of carbon dioxide between terrestrial plants and the atmosphere. In J. R. Ehleringer, A. Hall, & G. D. Farquhar (Eds.), *Stable isotopes and plant carbon-water relations* (pp. 47–70). Academic Press, Inc. <https://doi.org/10.1016/B978-0-08-091801-3.50011-8>
- Farquhar, G. D., Lloyd, J., Taylor, J. A., Flanagan, L. B., Syvertsen, J. P., Hubick, K. T., ... Ehleringer, J. R. (1993). Vegetation effects on the isotope composition of oxygen in atmospheric CO₂. *Nature*, 363, 439–443. <https://doi.org/10.1038/363439a0>
- Farris, F., & Strain, B. R. (1978). The Effects of water-stress on leaf H₂¹⁸O enrichment. *Radiation and Environmental Biophysics*, 15, 167–202. <https://doi.org/10.1007/BF01323264>
- Fiorella, R. P., Bares, R., Lin, J. C., Ehleringer, J. R., & Bowen, G. J. (2018). Detection and variability of combustion-derived vapor in an urban basin. *Atmospheric Chemistry and Physics*, 18(12), 8529–8547. <https://doi.org/10.5194/acp-18-8529-2018>
- Flanagan, L. B., Comstock, J. P., Ehleringer, J. R., Flanagan, L. B., Comstock, J. P., & Ehleringer, J. R. (1991). Comparison of modeled and observed environmental influences on the stable oxygen and hydrogen isotope composition of leaf water in *Phaseolus vulgaris* L. *Plant Physiology*, 96(2), 588–596. <https://doi.org/10.1104/pp.96.2.588>
- Frank, D. C., Poulter, B., Saurer, M., Esper, J., Huntingford, C., Helle, G., & Treydte, K. (2015). Water-use efficiency and transpiration across European forests during the Anthropocene. *Nature Climate Change*, 5, 579–584. <https://doi.org/10.1038/NCLIMATE2614>
- Friedman, I., Smith, G. I., Gleason, J. D., Warden, A., & Harris, J. M. (1992). Stable isotope composition of waters in southeastern California 1. Modern precipitation. *Journal of Geophysical Research*, 97(D5), 5795–5812. <https://doi.org/10.1029/92JD00184>
- Gat, J. (1996). Oxygen and hydrogen isotopes in the hydrologic cycle. *Annual Review of Earth and Planetary Sciences*, 24, 225–262. <https://doi.org/10.1146/annurev.earth.24.1.225>
- Gat, J. R., Bowser, C. J., & Kendall, C. (1994). The contribution of evaporation from the Great Lakes to the continental atmosphere: Estimate based on stable isotope data. *Geophysical Research Letters*, 21(7), 557–560. <https://doi.org/10.1029/94GL00069>
- Gaziz, C., & Feng, X. (2004). A stable isotope study of soil water: Evidence for mixing and preferential flow paths. *Geoderma*, 119, 97–111. [https://doi.org/10.1016/S0016-7061\(03\)00243-X](https://doi.org/10.1016/S0016-7061(03)00243-X)
- Gedney, N., Cox, P. M., Betts, R. A., Boucher, O., Huntingford, C., & Stott, P. A. (2006). Detection of a direct carbon dioxide effect in continental river runoff records. *Nature*, 439, 835–838. <https://doi.org/10.1038/nature04504>
- Good, S. P., Noone, D., & Bowen, G. (2015). Hydrologic connectivity constrains partitioning of global terrestrial water fluxes. *Science*, 349(6244), 175–178. <https://doi.org/10.1126/science.aaa5931>
- Good, S. P., Soderberg, K., Guan, K., King, E. G., Scanlon, T. M., & Caylor, K. K. (2014). δ²H isotopic flux partitioning of evapotranspiration over a grass field following a water pulse and subsequent dry down. *Water Resources Research*, 50, 1410–1432. <https://doi.org/10.1002/2013WR014333>
- Good, S. P., Soderberg, K., Wang, L., & Caylor, K. K. (2012). Uncertainties in the assessment of the isotopic composition of surface fluxes: A direct comparison of techniques using laser-based water vapor isotope analyzers. *Journal of Geophysical Research-Atmospheres*, 117(15), 1–22. <https://doi.org/10.1029/2011JD017168>
- Gough, C. M., Hardiman, B. S., Nave, L. E., Bohrer, G., Maurer, K. D., Vogel, C. S., ... Curtis, P. S. (2013). Sustained carbon uptake and storage following moderate disturbance in a Great Lakes forest. *Ecological Applications*, 23(5), 1202–1215. <https://doi.org/10.1890/12-1554.1>
- Granier, A. (1987). Evaluation of transpiration in a Douglas-fir stand by means of sap flow measurements. *Tree Physiology*, 3(4), 309–320. <https://doi.org/10.1093/treephys/3.4.309>
- Granier, A., & Loustau, D. (1994). Measuring and modelling the transpiration of a maritime pine canopy from sap-flow data. *Agricultural and Forest Meteorology*, 71, 61–81. [https://doi.org/10.1016/0168-1923\(94\)90100-7](https://doi.org/10.1016/0168-1923(94)90100-7)
- Haese, B., Werner, M., & Lohmann, G. (2013). Stable water isotopes in the coupled atmosphere-land surface model ECHAM5-JSBACH. *Geoscientific Model Development*, 6(5), 1463–1480. <https://doi.org/10.5194/gmd-6-1463-2013>
- Harwood, K. G., Gillon, J. S., Griffiths, H., & Broadmeadow, M. S. J. (1998). Diurnal variation of Δ¹³CO₂, Δ¹⁸O¹⁶O and evaporative site enrichment of δH₂¹⁸O in *Piper aduncum* under field conditions in Trinidad. *Plant, Cell and Environment*, 21(3), 269–283. <https://doi.org/10.1046/j.1365-3040.1998.00276.x>
- He, L., Ivanov, V. Y., Bohrer, G., Thomsen, J. E., Vogel, C. S., & Moghaddam, M. (2013). Temporal dynamics of soil moisture in a northern temperate mixed successional forest after a prescribed intermediate disturbance. *Agricultural and Forest Meteorology*, 180, 22–33. <https://doi.org/10.1016/j.agrformet.2013.04.014>
- Hendricks, S., Vande Kopple, R., Goodspeed, P., & White, D. (2016). Groundwater connectivity between Douglas Lake and Carp Creek based on fluorescein dye studies. *Michigan Academician*, 43(3), 380–392. <https://doi.org/10.7245/0026-2005-43.3.380>
- Hsieh, J. C. C., Chadwick, O. A., Kelly, E. F., & Savin, S. M. (1998). Oxygen isotopic composition of soil water: Quantifying evaporation and transpiration. *Geoderma*, 82, 269–293. [https://doi.org/10.1016/S0016-7061\(97\)00105-5](https://doi.org/10.1016/S0016-7061(97)00105-5)
- Hu, Z., Wen, X., Sun, X., Li, L., Yu, G., Lee, X., & Li, S. (2014). Partitioning of evapotranspiration through oxygen isotopic measurements of water pools and fluxes in a temperate grassland. *Journal of Geophysical Research - Biogeosciences*, 119, 358–371. <https://doi.org/10.1002/2013JG002367> Received
- Jackson, R. B., Carpenter, S. R., Dahm, C. N., McKnight, D. M., Naiman, R. J., Postel, S. L., & Running, S. W. (2001). Water in a

- changing world. *Ecological Applications*, 11(4), 1027–1045. [https://doi.org/10.1890/1051-0761\(2001\)011\[1027:WIACW\]2.0.CO;2](https://doi.org/10.1890/1051-0761(2001)011[1027:WIACW]2.0.CO;2)
- Jarvis, P. G., & McNaughton, K. G. (1986). Stomatal control of transpiration: scaling up from leaf to region. *Advances in Ecological Research*, 15, 1–49. [https://doi.org/10.1016/S0065-2504\(08\)60119-1](https://doi.org/10.1016/S0065-2504(08)60119-1)
- Jasechko, S., Sharp, Z. D., Gibson, J. J., Birks, S. J., Yi, Y., & Fawcett, P. J. (2013). Terrestrial water fluxes dominated by transpiration. *Nature*, 496(7445), 347–350. <https://doi.org/10.1038/nature11983>
- Ji, P., Yuan, X., & Liang, X.-Z. (2017). Do lateral flows matter for the hyper-resolution land surface modeling? *Journal of Geophysical Research-Atmospheres*, 122, 12077–12092. <https://doi.org/10.1002/2017JD027366>
- Keeling, D. (1958). The concentration and isotopic abundances of atmospheric carbon dioxide in rural areas. *Geochimica et Cosmochimica Acta*, 13, 322–334. [https://doi.org/10.1016/0016-7037\(58\)90033-4](https://doi.org/10.1016/0016-7037(58)90033-4)
- Kool, D., Agam, N., Lazarovitch, N., Heitman, J. L., Sauer, T. J., & Bengal, A. (2014). A review of approaches for evapotranspiration partitioning. *Agricultural and Forest Meteorology*, 184, 56–70. <https://doi.org/10.1016/j.agrformet.2013.09.003>
- Labat, D., Godd, Y., Probst, J. L., & Guyot, J. L. (2004). Evidence for global runoff increase related to climate warming. *Advances in Water Resources*, 27, 631–642. <https://doi.org/10.1016/j.advwatres.2004.02.020>
- Lai, C., Ehleringer, J. R., Bond, B. J., & Paw, K. (2006). Contributions of evaporation, isotopic non-steady state transpiration and atmospheric mixing on the $\delta^{18}\text{O}$ of water vapour in Pacific Northwest coniferous forests. *Plant, Cell & Environment*, 29, 77–94. <https://doi.org/10.1111/j.1365-3040.2005.01402.x>
- Lanning, M., Wang, L., Benson, M., Zhang, Q., & Novick, K. A. (2020). Canopy isotopic investigation reveals different water uptake dynamics of maples and oaks. *Phytochemistry*, 175(October 2019), 1–8. <https://doi.org/10.1016/j.phytochem.2020.112389>
- Lee, X., Kim, K., & Smith, R. (2007). Temporal variations of the $^{18}\text{O}/^{16}\text{O}$ signal of the whole-canopy transpiration in a temperate forest. *Global Biogeochemical Cycles*, 21(August), 1–12. <https://doi.org/10.1029/2006GB002871>
- Ling, M., Ping, L., Ping, Z., Xing-quan, R., Xi-an, C., & Xiao-ping, Z. (2008). Diurnal, daily, seasonal and annual patterns of sap-flux-scaled transpiration from an Acacia mangium plantation in South China. *Annals of Forest Science*, 65, 402–410. <https://doi.org/10.1051/forest:2008013>
- Lu, X., Liu, Z., An, S., Miralles, D. G., Maes, W., Liu, Y., & Tang, J. (2018). Potential of solar-induced chlorophyll fluorescence to estimate transpiration in a temperate forest. *Agricultural and Forest Meteorology*, 252(January), 75–87. <https://doi.org/10.1016/j.agrformet.2018.01.017>
- Lu, X., Liang, L. L., Wang, L., Jenerette, G. D., McCabe, M. F., & Grantz, D. A. (2017). Partitioning of evapotranspiration using a stable isotope technique in an arid and high temperature agricultural production system. *Agricultural Water Management*, 179, 103–109. <https://doi.org/10.1016/j.agwat.2016.08.012>
- Machavaram, M. V., & Krishnamurthy, R. V. (1995). Earth surface evaporative process: A case study from the Great Lakes region of the United States based on deuterium excess in precipitation. *Geochimica et Cosmochimica Acta*, 6(20), 4279–4283.
- Majoube, M. (1971). Oxygen-18 and deuterium fractionation between water and steam. *Journal of Chemical Physics*, 68, 1432–1436.
- Mao, J., Shi, X., Mao, J., Thornton, P. E., Forbes, W. L., Mao, J., ... Dickinson, R. E. (2015). Disentangling climatic and anthropogenic controls on global terrestrial evapotranspiration trends. *Environmental Research Letters*, 10(9), 1–14. 094008. <https://doi.org/10.1088/1748-9326/10/9/094008>
- Massmann, A., Gentine, P., & Lin, C. (2019). When does vapor pressure deficit drive or reduce evapotranspiration? *Journal of Advances in Modeling Earth Systems*, 11, 1–27. <https://doi.org/10.1029/2019MS001790>
- Matheny, A. M., Bohrer, G., Stoy, P. C., Baker, I. T., Black, A. T., Desai, A. R., ... Verbeeck, H. (2014). Characterizing the diurnal patterns of errors in the prediction of evapotranspiration by several land-surface models: An NACP analysis. *Journal of Geophysical Research - Biogeosciences*, 119(7), 1458–1473. <https://doi.org/10.1002/2014JG002623>
- Matheny, A. M., Bohrer, G., Vogel, C. S., Morin, T. H., He, L., Frasson, R. P. D. M., ... Curtis, P. S. (2014). Species-specific transpiration responses to intermediate disturbance in a northern hardwood forest. *Journal of Geophysical Research - Biogeosciences*, 119, 2292–2311. <https://doi.org/10.1002/2014JG002804>
- Matheny, A. M., Fiorella, R. P., Bohrer, G., Poulsen, C. J., Morin, T. H., Wunderlich, A., ... Curtis, P. S. (2017). Contrasting strategies of hydraulic control in two codominant temperate tree species. *Ecohydrology*, 10(3), 1–16. <https://doi.org/10.1002/eco.1815>
- Maxwell, R. M., & Condon, L. E. (2016). Connections between groundwater flow and transpiration partitioning. *Science*, 353(6297), 377–380. <https://doi.org/10.1126/science.aaf7891>
- McDonnell, J. J. (2014). The two water worlds hypothesis: ecohydrological separation of water between streams and trees? *Wiley Interdisciplinary Reviews Water*, 1(4), 323–329. <https://doi.org/10.1002/wat2.1027>
- Moreira, M., Sternberg, L., Martinelli, L., Victoria, R., Barbosa, E., Bonates, L., & Nepstad, D. (1997). Contribution of transpiration to forest ambient vapour based on isotopic measurements. *Global Change Biology*, 3(5), 439–450. <https://doi.org/10.1046/j.1365-2486.1997.00082.x>
- Mueller, B., Hirschi, M., Jimenez, C., Ciais, P., Dirmeyer, P. A., Dolman, A. J., ... Seneviratne, S. I. (2013). Benchmark products for land evapotranspiration: LandFlux-EVAL multi-data set synthesis. *Hydrology and Earth System Sciences*, 17, 3707–3720. <https://doi.org/10.5194/hess-17-3707-2013>
- Nave, L. E., Gough, C. M., Maurer, K. D., Bohrer, G., Hardiman, B. S., Le Moine, J., ... Curtis, P. S. (2011). Disturbance and the resilience of coupled carbon and nitrogen cycling in a north temperate forest. *Journal of Geophysical Research - Biogeosciences*, 116(4), 1–14. <https://doi.org/10.1029/2011JG001758>
- Ohmura, A., & Wild, M. (2002). Is the hydrological cycle accelerating? *Science*, 298, 1345–1347. <https://doi.org/10.1126/science.1078972>
- Penman, H. L. (1948). Natural evaporation from open water, bare soil and grass. *Proceedings Of The Royal Society of London Series A-Mathematical and Physical Sciences*, 193(1032), 120–145. <https://doi.org/10.1098/rspa.1948.0037>
- Phillips, N., & Oren, R. (1998). A comparison of daily representations of canopy conductance based on two conditional time-averaging methods and the dependence of daily conductance on environmental factors. *Annals of Forest Science*, 55, 217–235. <https://doi.org/10.1051/forest:19980113>
- Putman, A. L., Fiorella, R. P., Bowen, G. J., & Cai, Z. (2019). A global perspective on local meteoric water lines: Meta-analytic insight into fundamental controls and practical constraints. *Water Resources Research*, 55, 6896–6910. <https://doi.org/10.1029/2019WR025181>
- Quade, M., Brüggemann, N., Graf, A., Vereecken, H., & Rothfuss, Y. (2018). Investigation of kinetic isotopic fractionation of water during bare soil evaporation. *Water Resources Research*, 1978, 6909–6928. <https://doi.org/10.1029/2018WR023159>
- Schaeffer, S. M., Williams, D. G., & Goodrich, D. C. (2000). Transpiration of cottonwood/willow forest estimated from sap flux. *Agricultural and Forest Meteorology*, 105, 257–270. [https://doi.org/10.1016/S0168-1923\(00\)00186-6](https://doi.org/10.1016/S0168-1923(00)00186-6)
- Schlesinger, W. H., & Jasechko, S. (2014). Transpiration in the global water cycle. *Agricultural and Forest Meteorology*, 189–190, 115–117. <https://doi.org/10.1016/j.agrformet.2014.01.011>
- Scholl, M. A., Ingebritsen, S. E., Janik, C. J., & Kaauhikaua, J. P. (1996). Use of precipitation and groundwater isotopes to interpret regional hydrology on a tropical volcanic island: Kilauea volcano area, Hawaii. *Water*

- Resources Research*, 32(12), 3525–3537. <https://doi.org/10.1029/95WR02837>
- Scott, R. L., & Biederman, J. A. (2017). Partitioning evapotranspiration using long-term carbon dioxide and water vapor fluxes. *Geophysical Research Letters*, 44, 6833–6840. <https://doi.org/10.1002/2017GL074324>
- Shan, N., Ju, W., Migliavacca, M., Martini, D., Guanter, L., Chen, J., ... Zhang, Y. (2019). Modeling canopy conductance and transpiration from solar-induced chlorophyll fluorescence. *Agricultural and Forest Meteorology*, 268(February 2018), 189–201. <https://doi.org/10.1016/j.agrformet.2019.01.031>
- Simonin, K. A., Roddy, A. B., Link, P., Apodaca, R., Tu, K. P., Hu, J., ... Barbour, M. M. (2013). Isotopic composition of transpiration and rates of change in leaf water isotopologue storage in response to environmental variables. *Plant, Cell and Environment*, 36(12), 2190–2206. <https://doi.org/10.1111/pce.12129>
- Spangenberg, J. E. (2012). Caution on the storage of waters and aqueous solutions in plastic containers for hydrogen and oxygen stable isotope analysis. *Rapid Communications in Mass Spectrometry*, 26, 2627–2636. <https://doi.org/10.1002/rcm.6386>
- Sperry, J. S., Hacke, U. G., Oren, R., & Comstock, J. P. (2002). Water deficits and hydraulic limits to leaf water supply. *Plant, Cell & Environment*, 25, 251–263. <https://doi.org/10.1046/j.0016-8025.2001.00799.x>
- Starkenburg, D., Metzger, S., Fochesatto, G. J., Alfieri, J. G., Gens, R., Prakash, A., & Crisobal, J. (2016). Assessment of despiking methods for turbulence data in micrometeorology. *Journal of Atmospheric and Oceanic Technology*, 33, 2001–2013. <https://doi.org/10.1175/JTECH-D-15-0154.1>
- Stoy, P. C., El-madany, T. S., Fisher, J. B., Gentine, P., Gerken, T., & Good, S. P. (2019). Reviews and syntheses: Turning the challenges of partitioning ecosystem evaporation and transpiration into opportunities. *Biogeosciences*, 16, 3747–3775. <https://doi.org/10.5194/bg-16-3747-2019>
- Sulman, B. N., Roman, D. T., Scanlon, T. M., Wang, L., & Novick, K. A. (2016). Comparing methods for partitioning a decade of carbon dioxide and water vapor fluxes in a temperate forest. *Agricultural and Forest Meteorology*, 226–227, 229–245. <https://doi.org/10.1016/j.agrformet.2016.06.002>
- Sun, S., Meng, P., Zhang, J., Wan, X., Zheng, N., & He, C. (2014). Partitioning oak woodland evapotranspiration in the rocky mountainous area of North China was disturbed by foreign vapor, as estimated based on non-steady-state ^{18}O isotopic composition. *Agricultural and Forest Meteorology*, 184, 36–47. <https://doi.org/10.1016/j.agrformet.2013.08.006>
- Sutanto, S. J., Van Den Hurk, B., Dirmeyer, P. A., Seneviratne, S. I., Röckmann, T., Trenberth, K. E., ... Hoffmann, G. (2014). HESS opinions “a perspective on isotope versus non-isotope approaches to determine the contribution of transpiration to total evaporation.”. *Hydrology and Earth System Sciences*, 18(8), 2815–2827. <https://doi.org/10.5194/hess-18-2815-2014>
- Swann, A. L. S., Fung, I. Y., & Chiang, J. C. H. (2012). Mid-latitude afforestation shifts general circulation and tropical precipitation. *Proceedings of the National Academy of Sciences*, 109(3), 712–716. <https://doi.org/10.1073/pnas.1116706108>
- Talsma, C. J., Good, S. P., Jimenez, C., Martens, B., Fisher, J. B., Miralles, D. G., ... Purdy, A. J. (2018). Partitioning of evapotranspiration in remote sensing-based models. *Agricultural and Forest Meteorology*, 260–261, 131–143. <https://doi.org/10.1016/j.agrformet.2018.05.010>
- Tsujimura, M., Sasaki, L., Yamanaka, T., Sugimoto, A., Li, S., Matsushima, D., ... Saandar, M. (2007). Vertical distribution of stable isotopic composition in atmospheric water vapor and subsurface water in grassland and forest sites, eastern Mongolia. *Journal of Hydrology*, 333, 35–46. <https://doi.org/10.1016/j.jhydrol.2006.07.025>
- Tyree, M. T., & Zimmerman, M. H. (2002). *Xylem structure and the ascent of sap* (S.-V. N. Y. Inc. (ed.)). Springer.
- Vinukollu, R. K., Meynadier, R., Shef, J., & Wood, E. F. (2011). Multi-model, multi-sensor estimates of global evapotranspiration: Climatology, uncertainties and trends. *Hydrological Processes*, 25, 3993–4010. <https://doi.org/10.1002/hyp.8393>
- Wang, L., Caylor, K. K., Villegas, J. C., Barron-Gafford, G. A., Breshears, D. D., & Huxman, T. E. (2010). Partitioning evapotranspiration across gradients of woody plant cover: Assessment of a stable isotope technique. *Geophysical Research Letters*, 37(9), 1–7. <https://doi.org/10.1029/2010GL043228>
- Wang, L., Good, S. P., & Caylor, K. K. (2014). Global synthesis of vegetation control on evapotranspiration partitioning. *Geophysical Research Letters*, 41, 6753–6757. <https://doi.org/10.1002/2014GL061439>
- Wang, L., Good, S. P., Caylor, K. K., & Cernusak, L. A. (2012). Direct quantification of leaf transpiration isotopic composition. *Agricultural and Forest Meteorology*, 154–155, 127–135. <https://doi.org/10.1016/j.agrformet.2011.10.018>
- Wang, L., Niu, S., Good, S. P., Soderberg, K., McCabe, M. F., Sherry, R. A., ... Caylor, K. K. (2013). The effect of warming on grassland evapotranspiration partitioning using laser-based isotope monitoring techniques. *Geochimica et Cosmochimica Acta*, 111, 28–38. <https://doi.org/10.1016/j.gca.2012.12.047>
- Wang, P., Yamanaka, T., Li, X., & Wei, Z. (2015). Partitioning evapotranspiration in a temperate grassland ecosystem: Numerical modeling with isotopic tracers. *Agricultural and Forest Meteorology*, 208, 16–31. <https://doi.org/10.1016/j.agrformet.2015.04.006>
- Wang, X., & Yakir, D. (1995). Temporal and spatial variations in the oxygen-18 content of leaf water in different plant species. *Plant, Cell and Environment*, 18, 1377–1385. <https://doi.org/10.1111/j.1365-3040.1995.tb00198.x>
- Wang, X. F., & Yakir, D. (2000). Using stable isotopes of water in evapotranspiration studies. *Hydrological Processes*, 14(8), 1407–1421. [https://doi.org/10.1002/1099-1085\(20000615\)14:8<1407::AID-HYP992>3.0.CO;2-K](https://doi.org/10.1002/1099-1085(20000615)14:8<1407::AID-HYP992>3.0.CO;2-K)
- Webb, E. K., Pearman, G., & Leuning, R. (1980). Correction of flux measurements for density effects due to heat and water vapour transfer. *Quarterly Journal of the Royal Meteorological Society*, 106, 85–100. <https://doi.org/10.1002/qj.49710644707>
- Wei, Z., Yoshimura, K., Okazaki, A., Kim, W., Liu, Z., & Yokoi, M. (2015). Partitioning of evapotranspiration using high-frequency water vapor isotopic measurement over a rice paddy field. *Water Resources Research*, 51, 3716–3729. <https://doi.org/10.1002/2014WR016737>
- Wei, Z., Yoshimura, K., Wang, L., Miralles, D. G., Jasechko, S., & Lee, X. (2017). Revisiting the contribution of transpiration to global terrestrial evapotranspiration. *Geophysical Research Letters*, 44, 2792–2801. <https://doi.org/10.1002/2016GL072235>
- Welp, L. R., Lee, X., Griffis, T. J., Wen, X. F., Xiao, W., Li, S., ... Huang, J. (2012). A meta-analysis of water vapor deuterium-excess in the mid-latitude atmospheric surface layer. *Global Biogeochemical Cycles*, 26(3), 1–12. <https://doi.org/10.1029/2011GB004246>
- Wen, X., Yang, B., Sun, X., & Lee, X. (2016). Evapotranspiration partitioning through in-situ oxygen isotope measurements in an oasis cropland. *Agricultural and Forest Meteorology*, 230–231, 89–96. <https://doi.org/10.1016/j.agrformet.2015.12.003>
- West, A. G., Goldsmith, G. R., Brooks, P. D., & Dawson, T. E. (2010). Discrepancies between isotope ratio infrared spectroscopy and isotope ratio mass spectrometry for the stable isotope analysis of plant and soil waters. *Rapid Communications in Mass Spectrometry*, 24, 1948–1954. <https://doi.org/10.1002/rcm.4597>
- West, A. G., Patrickson, S. J., & Ehleringer, J. R. (2006). Water extraction times for plant and soil materials used in stable isotope analysis. *Rapid Communications in Mass Spectrometry*, 20, 1317–1321. <https://doi.org/10.1002/rcm.2456>
- Williams, D. G., Cable, W., Hultine, K., Hoedjes, J. C. B., Yezpe, E. A., Simonneaux, V., ... Chehbouni, A. (2004). Evapotranspiration components determined by stable isotope, sap flow and eddy covariance

- techniques. *Agricultural and Forest Meteorology*, 125, 241–258. <https://doi.org/10.1016/j.agrformet.2004.04.008>
- Wong, T. E., Nusbaumer, J., & Noone, D. C. (2017). Evaluation of modeled land-atmosphere exchanges with a comprehensive water isotope fractionation scheme in version 4 of the Community Land Model. *Journal of Advances in Modeling Earth Systems*, 9(2), 978–1001. <https://doi.org/10.1002/2016MS000842>
- Worden, J., Noone, D., & Bowman, K. (2007). Importance of rain evaporation and continental convection in the tropical water cycle. *Nature*, 445(February), 528–532. <https://doi.org/10.1038/nature05508>
- Wu, Y., Du, T., Ding, R., Tong, L., & Li, S. (2017). Multiple methods to partition evapotranspiration in a maize field. *Journal of Hydrometeorology*, 18, 139–149. <https://doi.org/10.1175/JHM-D-16-0138.1>
- Xiao, W., Lee, X., Hu, Y., Lui, S., Wang, W., Wen, X., ... Xie, C. (2017). An experimental investigation of kinetic fractionation of open-water evaporation over a large lake. *Journal of Geophysical Research-Atmospheres*, 122(11), 651–663. <https://doi.org/10.1002/2017JD026774>
- Xiao, W., Wei, Z., & Wen, X. (2018). Evapotranspiration partitioning at the ecosystem scale using the stable isotope method—A review. *Agricultural and Forest Meteorology*, 263(November 2017), 346–361. <https://doi.org/10.1016/j.agrformet.2018.09.005>
- Yakir, D., Berry, J. A., Giles, L., & Osmond, C. B. (1994). Isotopic heterogeneity of water in transpiring leaves: Identification of the component that controls the $\delta^{18}\text{O}$ of atmospheric O_2 and CO_2 . *Plant, Cell & Environment*, 17, 73–80. <https://doi.org/10.1111/j.1365-3040.1994.tb00267.x>
- Yakir, D., & Sternberg, S. L. (2000). The use of stable isotopes to study ecosystem gas exchange. *Oecologia*, 123, 297–311. <https://doi.org/10.1007/s004420051016>
- Yakir, D., & Wang, X.-F. (1996). Fluxes of CO_2 and H_2O between terrestrial vegetation and the atmosphere. *Nature*, 380, 515–517. <https://doi.org/10.1038/380515a0>
- Yepez, E. A., Huxman, T. E., Ignace, D. D., English, N. B., Weltzin, J. F., Castellanos, A. E., & Williams, D. G. (2005). Dynamics of transpiration and evaporation following a moisture pulse in semiarid grassland: A chamber-based isotope method for partitioning flux components. *Agricultural and Forest Meteorology*, 132, 359–376. <https://doi.org/10.1016/j.agrformet.2005.09.006>
- Yepez, E. A., Williams, D. G., Scott, R. L., & Lin, G. (2003). Partitioning overstory and understory evapotranspiration in a semiarid savanna woodland from the isotopic composition of water vapor. *Agricultural and Forest Meteorology*, 119(1–2), 53–68. [https://doi.org/10.1016/S0168-1923\(03\)00116-3](https://doi.org/10.1016/S0168-1923(03)00116-3)
- Zeng, Z., Piao, S., Li, L. Z. X., Wang, T., Ciais, P., Lian, X., ... Myneni, R. B. (2018). Impact of Earth greening on the terrestrial water cycle. *Journal of Climate*, 31, 2633–2650. <https://doi.org/10.1175/JCLI-D-17-0236.1>
- Zhang, Y., Peña-Arancibia, J. L., McVicar, T. R., Chiew, F. H. S., Vaze, J., Liu, C., ... Pan, M. (2016). Multi-decadal trends in global terrestrial evapotranspiration and its components. *Scientific Reports*, 6(19124), 1–12. <https://doi.org/10.1038/srep19124>
- Zhang, Y., Shen, Y., Sun, H., & Gates, J. B. (2011). Evapotranspiration and its partitioning in an irrigated winter wheat field: A combined isotopic and micrometeorologic approach. *Journal of Hydrology*, 408(3–4), 203–211. <https://doi.org/10.1016/j.jhydrol.2011.07.036>
- Zhou, S., Yu, B., Zhang, Y., Huang, Y., & Wang, G. (2016). Partitioning evapotranspiration based on the concept of underlying water use efficiency. *Water Resources Research*, 52, 1160–1175. <https://doi.org/10.1002/2015WR017766> Received
- Zhou, S., Yu, B., Zhang, Y., Huang, Y., & Wang, G. (2018). Water use efficiency and evapotranspiration partitioning for three typical ecosystems in the Heihe River Basin, northwestern China. *Agricultural and Forest Meteorology*, 253–254(February), 261–273. <https://doi.org/10.1016/j.agrformet.2018.02.002>

SUPPORTING INFORMATION

Additional supporting information may be found online in the Supporting Information section at the end of this article.

How to cite this article: Aron PG, Poulsen CJ, Fiorella RP, Matheny AM, Veverica TJ. An isotopic approach to partition evapotranspiration in a mixed deciduous forest. *Ecohydrology*. 2020;13:e2229. <https://doi.org/10.1002/eco.2229>